Remarks

At the time of the Office Action, claims 1-34 were pending in the subject application. Claims 7-11 and 24-33 were considered.

By this paper, claim 24 has been amended to recite a preparation having a medically efficacious substance coated with an aqueous liquid impermeable but gas permeable layer for surrounding and substantially preventing release of the medically efficacious substance, wherein the layer contains a ceramic, a clay, an inorganic non-metallic material, a polymer, a natural wax, a perforated stainless steel, or beeswax hardened with cornstarch and talc. With the deletion of several terms ("no medical change," "no chemical change," and "no diminution in its quantity in the preparation"), claim 24 in current form is believed to have been provided with greater clarity and requisite certainty in this regard. Claim 10 has been amended to correct a typographical error. Claims 25-28 and 30-33 have been amended to correct antecedent basis. Claim 36 is newly added to recite the preparation of claim 24 wherein the layer contains a wax in an amount of between 20% and 45% by weight of the preparation, a ceramic, or combinations thereof. Support for the amendment is found, *inter alia*, at lines 3-4 on page 7 and at lines 18-20 and 26-28 on page 20 of the specification as originally filed (unless otherwise noted, pages and lines cited in this paper are with reference to the specification as originally filed). In addition, claims 29 and 35 are canceled to advance prosecution. No new matter is introduced by these claim amendments.

Favorable consideration of pending claims 7-11, 24-28, 30-33 and 36 is respectfully requested.

Remarks Directed to the Earliest Effective Filing Date

The earliest effective filing date of the subject application is stated to be December 22, 2004 (Office Action, page 3). Applicant respectfully traverses this determination. The subject application is a national stage application from the corresponding PCT application

WO 2005/013942 having an international filing date of July 19, 2004. Therefore, the earliest effective filing date of the subject application should be no later than July 19, 2004, but **not** December 22, 2004 as stated. During a telephonic conversation with the Examiner Tigabu Kassa on April 3, 2009, the aforementioned correction with respect to the earliest effective filing date was acknowledged. Applicant respectfully request the Examiner to confirm the effective filing date of the subject application as no later than July 19, 2004 in the next Office communication.

Remarks Directed to Claim Rejections
under 35 U.S.C. § 101

The Examiner deems the Applicant's invention lacks patentable utility for failing to provide adequate evidence to support the utility to the invention (Office Action, page 3). In particular, the Examiner opines that "there is insufficient evidence to show that a compound which is not released on or into the body can have any medically beneficial effect" and that "the agents used to form the liquid impermeable but gas permeable layer (e.g. wax) are also used in the art to form controlled release formulations of drug." Applicant respectfully traverses this rejection.

In considering whether an application is "useful" under 35 U.S.C. § 101, the Patent Office is required to rely on the inventor's understanding of his invention and should focus on and be receptive to assertions made by the Applicant that an invention is useful."[1]

At the outset, it appears that the Examiner has approached examination of the Applicant's invention as though the invention was a new pharmaceutical and therefore referred to controlled release formulations. As will be discussed in more detail herein elsewhere, Applicant's claimed invention is neither a pharmaceutical nor a drug as conventionally known, but is a medical device eliciting therapeutical effects without being released into the blood circulation. In this regard, it would be beneficial to provide a brief description as to the discovery leading to and the features and the benefits of the Applicant's invention.

---

[1] MPEP 2107.01(1)

Applicant's invention can be used to reduce symptoms of and or to treat disorders associated with medical conditions characterized by blockage of exocrine glands including ducts of sweat glands (page 1, lines 4-7; page 4, lines 25-26).

Several disease conditions are related to the blockage of exocrine gland ducts. For example, blockage of sweat gland ducts lead to Miliaria, an acute inflammatory skin condition also known as Prickly Heat (page 1, lines 14-17). Miliaria occurs when sweat gland ducts are obstructed, however, the sweat glands continue to output fluid. Consequently, at just below the blockage site, the pressure of the sweat fluid ruptures the ducts and forces sweat into the surrounding skin (page 1, lines 23-27). In addition, it has been discovered that exocrine duct blockage on the head may similarly cause constriction or interruption of blood circulation and hence migraine (page 4, lines 8-10). It is, therefore, an object of the Applicant's invention to provide treatment for, or to reduce symptoms of, Miliaria and other similarly positioned disorders that are associated with exocrine malfunction (page 6, lines 9-10).

Claim 24 recites a preparation for use as a medicament, comprising a medically efficacious substance coated with an aqueous liquid impermeable but gas permeable layer for surrounding and preventing release of the medically efficacious substance, wherein the layer contains a ceramic, a clay, an inorganic non-metallic material, a polymer, a natural wax, a perforated stainless steel, or beeswax hardened with cornstarch and talc.

The medically efficacious substance of the claimed preparation is not intended to be released and dissolved into the blood stream, nor taken up by the body cells, nor subsequently metabolized to exert a downstream effect. Rather, when placed near to or against one's skin or placed intact in one's body, the claimed preparation and in particular the medically efficacious substance is in signaling communication with body's exocrine glands via gases in the surrounding environment. The communicating gases may include water vapor in the air and residual water vapor retained within the coating layer. In addition, as the coating layer is made aqueous liquid impermeable and hence hydrophobic, water vapor in the air tends to be attracted to the layer.

A non-limiting mechanism by which the claimed preparation functions as a medicament may be illustrated through its use to treat and or to reduce symptoms associated with the condition of hypertension in a patient. It is known that hypertension may be manifested by damages to skin capillary cells which are collectively called sweat ducts, a type of exocrine ducts. As a result of the damage, sweat ducts are blocked and life-saving electrolytes are not conserved. One of the benefits of the claimed preparation is to reduce or clear exocrine duct blockage such that physiologically normal capillary functions may be resumed. Since the capillary cells can regenerate in a period as short as 24 hours, a reduction of symptoms can be realized in an accordingly short period of time.

In certain particular embodiments, the medically efficacious substance is sodium chloride (NaCl) (page 6, lines 11-16). It is noted that sodium chloride is not conventionally regarded as medically efficacious, if ingested and passed into the blood stream. In fact, excess intake of sodium chloride rather induces, but not alleviates as is the case for the Applicant's invention, the onset of hypertension and other metabolic diseases. According to one or more embodiments of the Applicant's invention, sodium chloride is enclosed within the aqueous liquid impermeable but gas permeable layer such that sodium chloride is not released, nor digested, in the body.

The aqueous liquid impermeable but gas permeable layer of the Applicant's invention may be formed by hardening of beeswax with cornstarch and talc (page 8, line 21 to page 9, line 2). Such a layer is readily distinguished from prior art tablet coating formulations wherein wax is used to effect time-dependent release of pharmaceuticals. Prior art pharmaceutical formulations postpone release, but do not prevent the release of pharmaceuticals from a wax coating. As a result, the entire contents of the prior art formulations are eventually released, dissolved and metabolized in circulation, albeit a time-dependent manner.

It is discovered, according to one or more embodiments of the Applicant's invention, that an environment can be created for the body to sense a surplus of sodium chloride and to reset genetic habitations of the exocrine glands (page 15, lines 20-24).

Furthermore, to prevent desensitization of the body to sodium chloride and the wearing off of the therapeutic effect, the inventor found that treatment and prophylaxis have to be arranged so that the body can sense new additional sodium salt without absorbing it. Accordingly, sodium chloride used according to the Applicant's invention should be made neither to be released nor to cross epithelial barriers.

The environment indicating a surplus of sodium chloride can be a gaseous one in the case when the preparation is applied to one's external skin or can be a liquid one in the case when the preparation is placed intact in the gastrointestinal tract (GI tract) for a period of time prior to its fecal excretion (page 16, lines 15-18).

The claimed preparation, as placed in a body environment such as the one described hereinabove, but not in body circulation for cellular uptake and metabolism, may exert its function via influencing cell signaling and therefore delivering a desirable therapeutic effect without the substance having to be metabolized at all (page 16, lines 20-23).

In fact, one of the benefits provided by the claimed preparation is just to avoid the introduction of pharmaceuticals to enter one's blood circulation. Nearly all drugs in circulation have undesirable side effects at least since drugs in circulation may penetrate areas where they would be harmful, such as across the blood-brain barrier (page 18, lines 6-15).

Responsive to the above-quoted utility rejections with respect to effectiveness as a pharmaceutical, it seems the examiner has approached examination of the Applicant's invention as though the invention was a new pharmaceutical. It is absolutely agreed that a pharmaceutical could have no utility if no active substance was released into solution. However the Applicant's invention is not a pharmaceutical as defined and used conventionally. Rather, the claimed preparation can be categorized as a medical device according to the FDA: in relevant part, a device is:

> intended to affect the structure or any function of the body of man or other animals, and which ***does not*** achieve any of it's primary intended purposes through chemical action within or on the body of man or other animals and which is not

> dependent upon being metabolized for the achievement of any of its primary intended purposes.

This definition provides a clear distinction between a medical device and other FDA regulated products such as drugs or pharmaceuticals. Please see for instance Exhibit 1. The relevant test for a device is that the device is medically effective, that is to say that the device has a medical effect, even though it is not intended to be dissolved into the blood stream. The medical effect of the claimed preparation applied as a medical device is well shown in the examples given. Please see for instance, Example Four on pages 30-33.

Products according to one or more embodiments of the Applicant's invention have attained substantial commercial success. As stated in paragraph 17 of the Declaration of Warren Ward, the "Equiwinner" patches have been sold to professional horse trainers in various countries including the United States, United Kingdom, Australia and New Zealand. The retail selling price has been between 123 and 130 US dollars (or the equivalent) plus carriage and tax where applicable, for a box of ten patches, plus two spare patches.

As stated in paragraph 18 of the Declaration of Warren Ward, the "Equiwinner" patches according to the claimed invention have been very well received by the trainers, representing the only effective treatment known for the market. The total numbers of the "Equiwinner" patches sold in the last four consecutive calendar years were 5,000 patches, 11,000 patches, 18,000 patches, and 24,000 patches, with a market value of several hundred thousand dollars for year 2009. The magnitude of increase in sales is further reflective the high quality of the "Equiwinner" patches according to the claimed preparation. This secondary consideration strongly supports both utility and patentability of the claimed preparation.

The usefulness, under 35 U.S.C. § 101, of the Applicant's invention is believed to have been provided and further clarified according to the specification as filed and in light of the remarks set forth above.

Remarks Directed to Claim Rejections under 35 U.S.C. § 112

In rejecting claims 7-11, 24-28, and 30-33 under 35 U.S.C. § 112, the Examiner opines that "the specification does not enable . . . to ascertain the gas permeability of the coating layer . . . Applicant provides no evidence ... that the encapsulating layer is, in fact, gas permeable ... the only evidence for liquid impermeability ... is also for aqueous media and not for other liquids" (Office Action, page 4). Applicant respectfully traverses the rejections for at least the reasons set forth below.

With respect to liquid impermeability, claim 24 has been amended to recite an aqueous liquid impermeable but gas permeable layer. Therefore, objections or rejections to claim 24 for potentially lacking support for the layer's impermeability over other liquids are believed to have been obviated.

With respect to gas permeability, Applicant submits the following remarks, and in particular that gas permeability is inherent to the layer of the claimed preparation.

In at least one embodiment, the aqueous liquid impermeable but gas permeable layer is a wax matrix which is inherently gas permeable (page 20, lines 21-22). The gas permeability of the illustrated wax matrix coating layer is well known in the art such that testing is not done. The gas permeability property inherent to the wax matrix has many known extended uses, including to make fabrics breathable and to preserve freshness of citrus fruits by allowing ingress of air oxygen.

In at least another embodiment, the aqueous liquid impermeable but gas permeable layer contains a polymer (page 19, lines 26-27; and page 20, lines 23-24). The attached "Permeation of Gases and Vapours in Polymers" from the textbook "Polymer Permeability" ed. J. Comyn (Springer, 1985), concurrently submitted as Exhibit 2, explains at pages19-20 the reason that polymeric materials are inherently gas permeable.

In "Diffusion in and Through Polymers" (Wolf R. Vieth, 1991 Oxford University Press), concurrently submitted as Exhibit 3, is stated "[I]n strong contrast to gas penetration, polymer membranes may be highly swollen by a penetrating liquid, and their properties thus altered." The whole of the introduction to this book makes it clear that polymers are inherently gas permeable, and the quoted sentence illustrates that it is not difficult to ascertain by examination whether or not the polymer has been penetrated by water and swollen as a result. The sentence shows the clear difference between a membrane which has been hardened so as not to allow the passage of water but to only permit the passage of gas, and a membrane which has not been hardened so that liquids can pass.

"Tuning Nanoscopic Water Layers on Hydrophobic and Hydrophilic Surfaces with Laser Light" by Andrei P. Sommer, *et al.*, concurrently submitted as Exhibit 4, shows the way that nanoscopic interfacial water vapor permeates through the surface of hydrophobic materials, such as hardened polymers.

Moreover, U.S. Patent 5827538 "Osmotic Devices Having Vapor-Permeable Coatings", as cited by the Examiner, illustratively teaches that water vapor, which is a gas, permeates the polymer layers. This occurs naturally from atmospheric water vapor. No pressure, device or procedure is needed to have the water vapor permeate the layers. The wax or other polymer coating of the claimed preparation is permeated with water vapor and, in the case of sodium chloride, the sodium chloride within the coating is surrounded by water vapor. Sodium chloride does not dissolve in gas, only in liquid. The coating layer prevents ingress of liquid or egress of NaCl.

Therefore, for those in the art, knowledge of the permeability of polymer coatings is basic and essential. Many different types of such coatings are available from manufacturers who are able to provide technical information about permeability.

As stated, the claimed preparation is neither a pharmaceutical nor a drug. The word "drug" as referenced in Applicant's application is used to describe certain medically efficacious substances as drugs (please see at lines 6-9 on page 17 of the specification as

originally filed) suitable for encapsulation to form the claimed preparation. However the claimed preparation is not a drug, and the use of drugs within the encapsulation does not make the invention a drug. It is a medical device. The examples given are adequate to show the medical effect of the devices and to fully inform anyone skilled in the art in their formulation. The original specification at lines 5-10 on page 21 illustratively describes the testing needed to be done. Unlike those in the art wherein making pharmaceuticals are concerned with many parameters including dissolution, absorption, bioavability, metabolisation, elimination and so on, requiring extensive experimentation and therefore explanation and direction, these considerations do not necessarily apply to Applicant's invention. The encapsulated medically efficacious substance is not released or dissolved and is eliminated intact. Contrary to the assertion of the Examiner, the non-dissolution test is fully detailed at lines 5-10 on page 21 including the pH of the solutions. Whereas the standard dissolution test for pharmaceuticals lasts 15 minutes (FDA Dissolution Testing of Immediate Release Solid Oral Dosage Forms), concurrently submitted as Exhibit 6, the test specified at lines 5-10 on page 21 is carried out in a period of 27 hours. In addition to the 27 hour non-dissolution test specified herein, at lines 12-14 on page 21 is detailed the examination of a tablet recovered from faeces, the tablet being unchanged after use. This additional test easily confirms the integrity of the invention, in contrast to the practice in the case of pharmaceuticals where it is not possible to make this test. Details of testing are also given in the examples 1-3.

Therefore, and contrary to the Examiner's assertions cited herein, the Applicant's application has provided ample support to show that the aqueous impermeable but gas permeable layer can be made without any undue experimentation.

One example of the coating layer used in the claimed preparation is beeswax hardened with cornstarch and talc. Please see at lines 1-2 on page 9 of the original specification. The information given at lines 11-22 on page 20 is ample for any person skilled in the art to manufacture the invention. It will be apparent to anyone skilled in the art that the coating can firstly be made and tested. There are only two parameters, namely the quantity of cornstarch and talc to be used. A set of samples can be set up with incremental increases in the amounts of talc and cornstarch until it is estimated that the wax is just sufficiently hardened to

prevent dissolution. The set of coatings can then be applied to the active with the excipient ratio as given at lines 11-22 on page 20 of the original specification at between 20% and 45% by weight. The resulting samples may then be tested as described at lines 5-10 on page 21 of the original specification. For a person skilled in the art, the number of samples is unlikely to exceed ten in number, and the entire experimentation is unlikely to exceed 12 hours bench time plus the 27 hours liquid impermeability testing mentioned herein elsewhere.

It may reasonably occur to any skilled artisan to include with the medically efficacious substrate a low level of water soluble food dye, such as carmine red, as an indicator for any release of the substance. If a formulation did not release the, dye that would be a first indication that the active is satisfactorily retained within the dosage form. It would then reasonably occur to any investigator in the art to investigate the water solutions used for testing for any presence of the active. Therefore, the subject application has provided ample support to show the coating layer be made and used water impermeable.

It appears that the Examiner has referred to controlled release formulations. US Patent 4126672 "Sustained Release Pharmaceutical Capsules" illustrates factors which govern the controlled release formulations. While conventionally pharmaceuticals may require more extensive experimentation with regard to controlled dosage forms, these aspects of experimentation are simply not substantially relevant to practice the Applicant's invention.

Using commercially available polymers is also simple. For example Eudragit RS 30 D is a well known polymethacrylate resin used for coating tablets, including controlled release tablets. Please see for instance Exhibit 7. The manufacturers (EVONIK Röhm GmbH, Pharma Polymers, Darmstadt, Germany) specify the addition of 6% of Triethyl Citrate to the resin in water. The manufactures specify a number of tests, well known to those in the art, for testing for film formation. In the case of the instant invention the only remaining parameter for successful non-dissolution of a coated substance is the amount of hardener to be added to the coating solution. Talc is a suitable hardener and is well known to be used as such. 25% to 30% by weight is a suitable amount of talc and it is unlikely that a formulation scientist would take more than a day to arrive at a value within this ratio. With polymer-coating for sustained

release oral dosage forms, drug release through the polymer membrane is diffusion controlled. The diffusion is thereby dependent on the membrane permeability, which is seen as directly connected to the water uptake or swelling, respectively, of the polymer membrane. (Sutter B., et al Polymerfilme als Diffusionsbarrieren für perorale Retardarzneiformen unter besonderer Berücksichtigung wässriger Dispersionen. Acta Pharm Technol. 1988;34:179-188.) In the case of the Eudragit polymer plus talc as above, the addition of the talc hardening the polymer prevents the liquid water uptake, but the polymer retains its inherent property, permeability to gas (in this case water vapour), as is well known to any person skilled in the art. (Also see "Permeation of Gases and Vapours in Polymers" above)

Therefore, contrary to the Examiner's assertions, making the aqueous liquid impermeable but gas permeable layer is well known in the art. ***What is conventional or well known to one of ordinary skill in the art need not be disclosed in detail.***[2] Reconsideration and withdrawal of this rejection is solicited.

In rejecting claims 7-11, 24-33 and 35 under 35 U.S.C. § 112, the Examiner further opines that the specification does not provide enablement for how to use the claimed preparation for the treatment of diseases because the coated substance is not released (Office Action, pages 4-5).

The Examiner correctly admits that the prior art fails to teach or suggest the claimed preparation, wherein the medically efficacious material such as NaCl is not released, would be efficacious at all (Office Action, pages 6-7).

In response, Applicant incorporates by reference all remarks stated herein in relation to the utility rejection and submit, in addition, the following remarks.

---

[2] See *Hybritech Inc. v. Monoclonal Antibodies, Inc.*, 802 F.2d at 1384, 231 USPQ at 94. See also *Capon v. Eshhar*, 418 F.3d 1349, 1357, 76 USPQ2d 1078, 1085 (Fed. Cir. 2005). See also MPEP 2163II3(a).

In his 2003 Nobel lecture "Potassium channels and the atomic basis of selective ion conduction" (concurrently submitted as Exhibit 5), Roderick MacKinnon reported the discovery of the architecture and action of potassium ion (K^+) channels applicable to all fauna, and stated that sodium (Na^+) ion channels worked in the same way. These ion channels are found in all cells of the human body and other mammals. It is clear from this his paper that the proximity of a potassium ion to a cell causes electrical activity in the ion channel. One or more embodiments of Applicant's invention allow for sodium chloride and other medically efficacious substances to be placed in close proximity to body cells, and thus ion channels, the sodium chloride or other substances being surrounded by water vapour. Further water vapour, in the case of skin patches, or liquid water, in the case of ingested products, surrounds the coated invention. With reference to Figure 7 of the paper, MacKinnon explains that electron density (blue mesh) for K+ ions in the filter and for a K+ ion and water molecules in the central cavity are shown. White lines highlight the coordination geometry of K+ in the filter and in water.

In other words, the ion channel recognizes not the ion but the pattern of liquid molecules and particularly water molecules around the ion. So in the instance wherein the claimed preparation is applied as a pill passing through the GI tract in close proximity to epithelial cells causes cell ion channels to open in anticipation of receiving ions. A plurality of electrical signals can be signified by the pattern changes in the surrounding environment generated by the opening of the ion channels as the pill moves along. Alternatively, in the instance wherein the claimed preparation is applied as the skin patches, there is no movement which is one reason why each of the patches uses two granules on the patch. Please see at line 22 on page 11 to line 2 on page 12 of the specification as originally filed. This arrangement provides that dermal ion channels are opened on a flip-flop basis, mimicking of movement achieving the same effect as that of the pill. The activation of ion channels as explained above is a medical effect produced by a substance which is not released. Please see also at line 8 on page 14 to line 23 on page 16 of the specification as originally filed.

For the reasons set forth above, Applicant believes that the claimed invention is enabled. Reconsideration and withdrawal of rejections to claims 7-11, 24-28, and 30-33 under 35 U.S.C. 112, first paragraph, is respectfully solicited.

Remarks Directed to Claim 36

Claim 36 is newly added to recited the preparation of claim 24, wherein the coating layer contains a wax in an amount of between 20% and 45% by weight of the preparation, a ceramic, or combinations thereof. Support for the amendment is found, *inter alia*, at lines 17-22 of the specification originally filed.

The claimed preparation of claim 36, which contains a relatively high content of wax in a range of 20% to 45% by weight for liquid impermeability, clearly departs from the conventional art which uses only a minimal amount of wax, e.g., in a range of 1% to 5% by weight, to facilitate but not to inhibit the release of drug components although in a delayed formulation.

Allowability of claim 36 is solicited.

Conclusion

Applicant submits that the claims are now in condition for allowance, and respectfully requests a Notice to that effect. If the Examiner believes that further discussion will advance the prosecution of the application, the Examiner is highly encouraged to telephone Applicant's attorney at the number given below.

Please charge any fees or credit any overpayments as a result of the filing of this paper to our Deposit Account No. 02-3978.

Respectfully submitted,

WARREN WARD

By /Junqi Hang/
Junqi Hang
Reg. No. 54,615
Attorney/Agent for Applicant

Date: April 7, 2009

BROOKS KUSHMAN P.C.
1000 Town Center, 22nd Floor
Southfield, MI 48075-1238
Phone: 248-358-4400
Fax: 248-358-3351

EXHIBIT 1

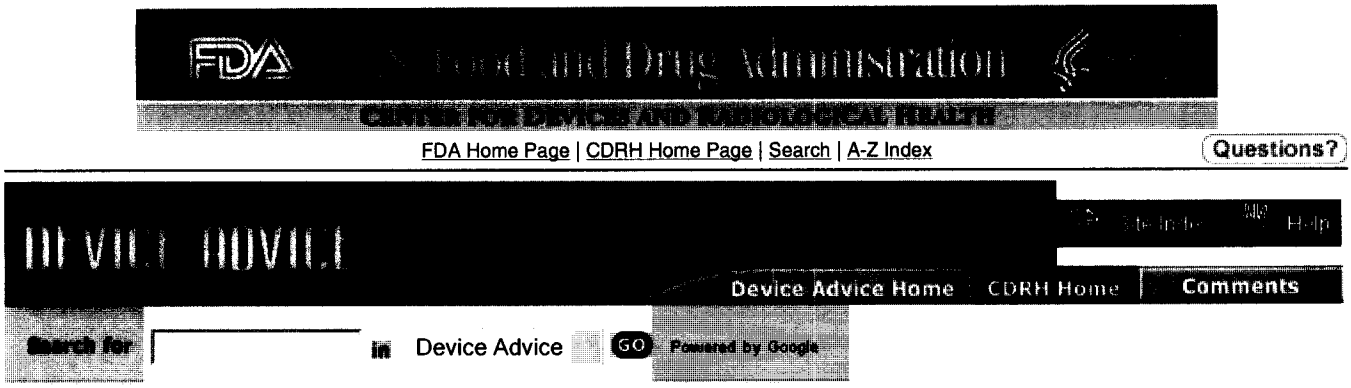

Please note: as of October 1, 2002, FDA charges fees for review of Premarket Notification 510(k)s and Premarket Approvals

Is The Product A Medical Device?

Introduction

Determine if your product meets the Definition of a device. If it does, there are FDA requirements that apply. First, see the definition below.

Medical Device Definition

Medical devices range from simple tongue depressors and bedpans to complex programmable pacemakers with micro-chip technology and laser surgical devices. In addition, medical devices include in vitro diagnostic products, such as general purpose lab equipment, reagents, and test kits, which may include monoclonal antibody technology. Certain electronic radiation emitting products with medical application and claims meet the definition of medical device. Examples include diagnostic ultrasound products, x-ray machines and medical lasers. If a product is labeled, promoted or used in a manner that meets the following definition in section 201(h) of the Federal Food Drug & Cosmetic (FD&C) Act it will be regulated by the Food and Drug Administration (FDA) as a medical device and is subject to premarketing and postmarketing regulatory controls. A device is:

- "an instrument, apparatus, implement, machine, contrivance, implant, in vitro reagent, or other similar or related article, including a component part, or accessory which is:
  - recognized in the official National Formulary, or the United States Pharmacopoeia, or any supplement to them,
  - intended for use in the diagnosis of disease or other conditions, or in the cure, mitigation, treatment, or prevention of disease, in man or other animals, or
  - intended to affect the structure or any function of the body of man or other animals, and which does not achieve any of it's primary intended purposes through chemical action within or on the body of man or other animals and which is not dependent upon being metabolized for the achievement of any of its primary intended purposes."

This definition provides a clear distinction between a medical device and other FDA regulated products such as drugs. If the primary intended use of the product is achieved through chemical action or by being metabolized by the body, the product is usually a drug. Human drugs are regulated by FDA's Center for Drug Evaluation and Research (CDER). Biological products which include blood and blood products, and blood banking equipment are regulated by FDA's Center for Biologics Evaluation and Research (CBER). FDA's Center for Veterinary Medicine (CVM) regulates products used with animals. If your product is not a medical device but regulated by another Center in the FDA, each component of the FDA has an office to assist with questions about the products they regulate. In cases where it is not clear whether a product is a medical device there are procedures in place to use DSMICA Staff Directory to assist you in making a determination.

Check the Precedent Correspondence (Previous decisions on products) for information on a related product that may assist

you in determining the requirements you need to consider for your product.

Updated February 28, 2002

Choose another topic: Select a topic

Accessibility Disclaimer

EXHIBIT 2

Chapter 2

Permeation of Gases and Vapours in Polymers

C. E. ROGERS

Department of Macromolecular Science, Case Western Reserve University, Cleveland, Ohio, USA

1. INTRODUCTION

The solution and transport behaviour of low molecular weight substances in polymeric materials is a topic of interest for many fields of science and technology. The importance and relevance of such behaviour has become more apparent in recent years with the accelerating development of separation membrane systems, highly impermeable or selectively permeable packaging or barrier films, and the overall increase in the use of polymeric materials for diverse applications with consequent exposure to various environmental agents.

The selection or development of polymeric materials for use in applications with stringent design specifications relating to their solution and transport behaviour requires knowledge and appreciation

diffusion behaviour, often observed in biological systems, is related to the directional flux effects observed in systems with a polymer membrane possessing a gradient of chemical composition,[43–46] or temperature, or stress, or other variable which affects diffusion in terms of irreversible thermodynamics.

The transport of a penetrant through a homogeneous membrane, in the absence of gross defects such as pores or cracks, is usually considered to occur by the following process: solution (condensation and mixing) of the gas or vapour in the surface layers, migration to the opposite surface under a concentration (chemical potential) gradient, and evaporation from that surface into the ambient phase. The migration of the penetrant can be visualised as a sequence of unit diffusion steps or jumps during which the particle passes over a potential barrier separating one position from the next.

The unit diffusion or jump involves a cooperative rearrangement of the penetrant molecule and its surrounding polymer chain segments. It is not necessary that a 'hole' *per se* be formed in the polymer structure between two successive penetrant positions (although this is often the basis for model calculations); the penetrant molecule and its surrounding chain segments may share some common volume before and after the diffusion jump. However, a certain number of van der Waals type or other interactions between the component molecules and chain segments must be broken to allow a rearrangement of the local structure. The amount of energy required for this rearrangement (or 'hole formation') will increase as the size and shape of the penetrant molecule increase. Several jumps may need to occur in the same direction before the molecule has been displaced by a distance equal to its size.

This process requires a localisation of energy to be available to the diffusing molecule and its polymer chain segment neighbours to provide the energy needed for rearrangement against the cohesive forces of the medium with effective movement of the penetrant for a successful jump. In a polymer above its glass temperature, as in simple liquids, fluctuations in density ('holes') are constantly disappearing and reforming as a result of thermal fluctuations. Low density regions resulting from an outward expansion of chain segments from a central point can be associated with a localised accumulation of energy causing the expansion.

Diffusive motion thus depends on the relative mobilities of penetrant molecules and polymeric chain segments as they are affected by

changes in size, shape, concentration, component interactions, temperature and other factors which affect polymeric segmental mobility. Since diffusion requires rearrangement of the relative molecular conformations within a mixture, the behaviour is closely related to the rheological and mechanical properties of the solid in the presence of penetrant. In many cases, relatively long-term relaxation processes may delay the rate of approach to equilibrium with consequent marked effect on concurrent diffusion and solution behaviour.

Studies of concurrent solution/diffusion and stress relaxation or creep in a given system can be used to advantage for elucidating the nature of polymer chain segmental motions as they affect both viscoelastic and transport behaviours.[4,87–90] However, it must be emphasised that the molecular and segmental motions are somewhat different for the two processes, especially when diffusion is compared with the bulk viscosity of the polymer. For the diffusion of small molecules only relatively local coordination of segmental motions are involved. In viscous flow processes, there is an actual displacement of polymer molecules requiring more coordination of these segmental motions. The two processes utilise different spectra of the distribution of segmental motions (or free volume fluctuation distribution). It is to be expected that any correlation between the processes will be closer for low penetrant concentrations or large-size penetrants where the segmental motions involved in the two processes are more nearly equivalent.

The overall transport process in a polymer therefore depends on two major factors which, in turn, are governed by a wide variety of factors related to composition, fabrication and experimental conditions. One factor is polymer chain segmental mobility and the other is defect structures, such as voids, microcracks and other non-thermodynamic variations in polymer structure and morphology. Defect structures are usually difficult to either define or characterise, but their effect on transport and solution behaviour can be profound. Gross defects, such as pinholes and cracks, are of great experimental concern but are not to be considered here since their effects on transport are overwhelming and usually obvious to the investigator—the film leaks profusely. It is the smaller defects which give more subtle, but important, contributions to the overall transport and solution processes that we need to consider. These include spherulitic and lamellar boundary regions in semi-crystalline polymers and permanent or transient voids (excess free volume, 'frozen holes', etc.) found in glassy polymers.

EXHIBIT 3

1

OVERVIEW

1.0 INTRODUCTION

In recent years, there has been a rapid increase in the number and variety of challenges and opportunities facing practitioners of chemical engineering and applied chemistry in the areas of permeability-controlled devices and processes. Conventional techniques are insufficiently flexible or too costly in many cases, and advanced processes are being developed to meet new needs.

One of the most interesting of the applications of the principles of ***diffusion in and through polymers*** is the use of selective permeation through membranes to effect separations. Two aspects of the field logically emerge and are addressed here: the basic nature of the transport process itself and the engineering factors important in achieving successful designs, varying from small-scale appliances to large-scale industrial operations. The former has been accorded considerable attention in the published literature, and the latter is being given increasing attention. One purpose of this book, then, is to examine the present state of the art with respect to interrelated scientific and engineering aspects, expanding the latter to include consideration of bioprocess applications, such as those encountered with biosensors, controlled release, and bioreactors.

In order to understand the mechanisms of transport in the various polymers of interest, it is useful to consider features of the two principal microstructural conditions of polymeric materials: the glassy and rubbery states. In the glassy state, a polymer is hard and may be brittle, these properties being intimately related to restricted polymer chain mobility. Rotation about the chain axis is limited and motion within the structure is largely vibratory within a frozen quasi-lattice. Polymers of this type are very dense structures, with very little internal void space (ca. 2 to 10%). Hence, it is not surprising that penetrant diffusivities through such a structure are low but that discrimination between penetrants on the basis of size is excellent. Glassy behavior is

associated with chain stiffness, strong intermolecular forces between backbone chains, and the presence of bulky side groups.

In contrast, polymers in the rubbery state typically are tough and flexible, with such properties associated with freer chain motion. In this case, larger segments are thought to participate in the diffusion process due to internal micromotions of chain rotation and translation, as well as vibration. Basically, then, a larger amount of free volume in which diffusion may take place is more readily accessible.

In both glassy and rubbery states, these properties can be further modified by the presence of a crystalline phase, or by stress-induced orientation. Both crystallization and orientation tend to place additional constraints on the mobility of the amorphous phase through which diffusion takes place. Also, the crystalline phase is usually impermeable, which results in longer and more tortuous diffusion paths.

Focusing for a moment on the topic of glassy polymers per se, their inherent versatility places them among the most important materials of the present time. As a result, scientific and technological investigations involving the triadic relationship between structure, property and function, or application, for polymeric glasses have increasingly become a common mode for research workers. As has been observed, the behavior of the properties of a polymeric material at a temperature below the glass transition region can be quite complex and also rather unique. Much of this pattern has been ascribed to the nonequilibrium nature of the structurally-arrested glassy state, with properties generally and appropriately characterized as history-dependent and time-dependent.

From a practical point of view, a better understanding of the

From a practical point of view, a better understanding of the nonequilibrium molecular characteristics of the glassy state and their effects on the properties and applications of glassy polymers is deemed crucial in improving the predictability of the performance of a material to optimize its end-uses. From a theoretical point of view, deeper understanding will assist in consolidating the framework required for the attainment of a unified picture of the glassy state and a sound theory or model capable of fully describing its complex behavior. Hence, the inherent nonequilibrium structure of the glassy state and its effects on the properties and functions of glassy polymers continues to be of lively interest to researchers, as will become apparent throughout this book.

It is generally not such a simple task to select the appropriate types of experiments whose results will impart meaningful understanding regarding the intimate link between structural changes and the direct consequence involving a certain property, functionality or prac-

tical application. This link or interrelationship may often seem somewhat ambiguous, for a variety of properties and practical end-uses. The difficulty is further compounded by the relative paucity of analytical means to examine the microstructure of an amorphous polymeric material per se, or at least to detect a structural change at the microscopic level. Conventional and available experimental techniques such as x-ray analysis are sometimes not of major benefit, other than to show that the material is free of crystallites, confirming the assumed amorphous structure. It is encouraging to note that sophisticated resonance techniques such as NMR or ESR (electron-spin resonance) are coming into play for the elucidation of the interaction of penetrants with glassy polymer microstructures. Mikhailov and Kuzina (1990) observed what they termed micro- and macro-diffusion in polystyrene, related to the kinetic inhomogeneity of the matrix which resulted in a wide spectrum of activational barriers (ca. 5-20 kcal/mol). Cain et al. (1989) employed NMR spin relaxation experiments to show that the translational diffusion coefficients of CO_2 in silicone rubber have a wide distribution, and the self-diffusion coefficients span a range of nearly four orders of magnitude (10^{-10} to 10^{-6} cm^2/s) at ca. 300K. The small fraction of the CO_2 with diffusion coefficients of 10^{-6} to 10^{-4} cm^2/s apparently reflects those channels suitable for rapid transport of CO_2 through the rubber. In studies of Xe diffusion in bisphenol A polycarbonate, a distribution of relaxation times arising from the inhomogeneous character of the polymeric matrix is observed. Ohno and Suzuoki (1986) have applied broad-line NMR spectroscopy to develop a new quantitative parameter, $(\Delta H^2)_{inter}$, to describe the packing state of polymers. In this way, the intermolecular terms of the second moment are found to correlate well with membrane gas permeability coefficients.

heights.

As has been pointed out in a host of more recent studies within the last decade, the nonequilibrium nature of the glassy state may be surfacing or mechanistically partaking in the behavior of a polymer throughout its existence. Thus, the perturbation may well be occurring either during a processing cycle or within the service lifetime of a polymer. Besides thermal annealing, other types of perturbations such as static mechanical pressure, tensile strain, or even exposure to a gaseous substance could result in - or could lead to - a complex response which may in fact be a nonequilibrium or glassy one. The specific manner whereby a disturbance is introduced could also play an important role.

The effects of exposure of glassy polymers to small molecules are of particular interest to chemical engineers, since many of their in-

volvements with polymer applications include sorption and transport of permanent gases. For instance, Langsam and Robeson (1989) recently reported on the effects of oxygen partial pressure and temperature on the lifetime of polymer films used in gas separation processes studied by a combination of test procedures based on thermogravimetric analysis and mechanical properties. The use of commercial antioxidants increased the temperature at which the film was usable in a separation process. The decline in permeability during accelerated aging was associated with a chain scission process and an embrittlement of the film. The lifetime of the protected films at ambient conditions (25°/170 mm O_2) was greater than five years. The flux decline was due to the contamination of films with hydrocarbon vapor. Water vapor had no effect on the permeabilities or the selectivity of the gas pair, O_2/N_2, in surface-fluorinated polymer films.

Indeed, the examination of sorption and transport properties of small molecules in polymeric materials has long been known to be a promising means to progress toward the goal of a unified concept along one main avenue. Having already obtained a reasonable degree of success in interpreting the microstructure of semicrystalline and glassy polymers via these properties, the use of small molecules as microstructural probes is being more and more enthusiastically adopted by chemical engineers and chemists who are involved in applied research on polymeric materials, in search of polymer microstates with superior membrane selection and/or retention properties for industrial and biomedical applications. In following the advances which have been achieved by these workers, the transport portion of the ultimate triadic relationship appears to be naturally attainable since many of the practical applications and end-uses of glassy polymers involve sorption and transport of small molecules as fundamental processes. These include a wide variety of applications, ranging from small scale uses such as packaging materials for consumer products and protective coatings, to large scale industrial processes such as permselective membranes for gas separations (Dao, 1989).

1.1 GAS PERMEATION

In the permeation of non-condensible gases in polymeric membranes, equilibrium levels of gas sorption in the solid are low because interactions between solute molecules and the polymer are weak. Diffusion constants are independent of penetrant concentration in the membrane. Application of Fick's law and Henry's law results in a

transport equation in which the flux rate is given by the product of a new constant, the permeability, and the partial pressure gradient across the membrane. In this case, the permeability is the product of the diffusivity and the Henry's law constant. It has been found that the permeability varies with temperature according to an Arrhenius-type equation. The apparent activation energy for permeation is the sum of a diffusion activation energy and the enthalpy of solution, each in turn related to the temperature dependence of diffusivity and solubility.

Because of limited polymer chain mobility, penetrant molecular size and shape are important parameters in determining the diffusion coefficient. Indeed, it is this capacity of a polymeric membrane to discriminate between penetrants with subtle steric differences that contributes significantly to membrane selectivity and ultimate value in a separations process. A second important factor is the chemical similarity between penetrant and polymer. The qualitative solubility rule of " like dissolves like" is obeyed. Thus, gas molecules which have a solubility parameter close to that of the membrane material will tend to be more soluble, possibly resulting in higher fluxes.

Where specific interactions between penetrant and polymer become important, such as when hydrogen bonding is involved, the relationship among diffusivity, solubility, and measured permeability is more complicated. Permeation of solvating vapors, such as, for example, water in ethyl cellulose and many hydrocarbons in polyethylene, shows a concentration dependence of both diffusivity and solubility.

1.2 LIQUID AND VAPOR PERMEATION

Liquid permeation involves the solution of liquid at the upstream face of the membrane, followed by diffusion through the membrane, and desorption from the downstream face. In strong contrast to gas permeation, polymer membranes may be highly swollen by a penetrating liquid, and their properties thus altered. For liquids in polymers, sorbed volumes can be 10 to 20% or even higher, compared to gas-polymer systems where sorbed volumes are vanishingly small in most cases. Thus, liquids open up the structure, with the result that the absolute flux rates through the membrane can be 2 to 3 orders of magnitude higher for a liquid than for a noncondensible gas.

However, similar ideas which are useful in describing the "ideal" behavior of gas-polymer solutions can be modified to describe the liquid permeation process. The transport equation is again based on

Fick's law but diffusion coefficients are strong functions of concentration (typically exponential). Since the driving force is the concentration of dissolved liquid, liquid solubility in the polymer brings in the relationship between chemical structure of penetrant and membrane.

Diffusion constants, apart from their concentration dependence, also depend on molecular size and shape, and as in gas permeation, crystallinity and orientation have important effects on the transport process. In the presence of a swelling liquid, crystalline polymer membranes actually undergo structural rearrangements as a result of the interactions between penetrant and polymer. At these levels of sorption, sufficient liquid is present within the polymer phase to depress the melting point of crystals, and thus generate changes in the crystalline size and texture of an organic polymer. In fact, this process can be used to advantage to "tailor" membranes and a body of literature has developed from attempts to increase the selectivity of membrane separation by such methods.

1.3 REVERSE OSMOSIS

In a closed system with pure solvent separated from a solution by a membrane permeable to solvent only, solvent will flow into solution in the direction of decreasing solvent activity by a process known as osmosis. If the activity of solvent in solution is raised above its level in the pure state at one atmosphere, such as by application of hydrostatic pressure, net solvent flow will proceed from solution to pure solvent, a process which has been named reverse osmosis. Thus, applying a hydrostatic pressure in excess of the osmotic pressure to an aqueous salt solution in contact with a hydrophilic membrane will result in

Author:
Prof. Wolf R. Vieth
College of Engineering, Rutgers University, Piscataway NJ 08854 USA

Distributed in USA and in Canada by
Oxford University Press
200 Madison Avenue, New York, N. Y. 10016

Distributed in all other countries by
Carl Hanser Verlag
Kolbergerstraße 22
D-8000 München 80

CIP-Titelaufnahme der Deutschen Bibliothek
Vieth, Wolf R.:
Diffusion in and through polymers : principles and applications / Wolf R. Vieth. - Munich : Vienna ; New York ; Barcelona : Hanser ; New York ; Don Mills, Ontario : Oxford Univ. Press, 1991
ISBN 3-446-15574-0

ISBN 3-446-15574-0 Carl Hanser Verlag Munich Vienna New York Barcelona
ISBN 0-19-520906-0 Oxford University Press

Cover art after R. J. Pace and A. Datyner,
J. Polym. Sci., Polym. Phys. Ed., 17, 437-51 (1979).

Cover design: Kaselow Design, Munich
Printed in Germany by Grafische Kunstanstalt Josef C. Huber KG, Dießen

EXHIBIT 4

Tuning Nanoscopic Water Layers on Hydrophobic and Hydrophilic Surfaces with Laser Light

Andrei P. Sommer,*,† Arnaud Caron,† and Hans-Joerg Fecht†,‡

Institute of Micro and Nanomaterials, University of Ulm, 89081 Ulm, Germany, and Institute for Nanotechnology, Forschungszentrum Karlsruhe, 76021 Karlsruhe, Germany

Received October 20, 2007. In Final Form: November 27, 2007

The evolutional function of ordered interfacial water near solid surfaces was postulated by Szent-Györgyi: "Life actually, may have started with building these water structures." Here we report their tunability with laser light on both hydrophobic and hydrophilic surfaces. On the former, the light caused their depletion—on the latter, an increase in fluidity—as measured by atomic force acoustic microscopy. Interfacial water layers play a key role in cellular recognition. Their tunability promises to revolutionize various fields in biomedical engineering and life sciences.

The biochemical and biological implications of ordered nanoscopic water layers are enormous. Presumably, they not only mask proteins, thereby modifying their reactivity,[1] but also play the role of informational blueprints in first contact events in cell−cell and cell−material contacts.[2] One of the pioneering investigations indicating the prevalence of ordered nanoscopic water layers on solid surfaces exposed to air has been conducted exemplarily on hydrophobic polymers.[3] By using a near-field scanning optical microscope (NSOM), it was shown that the profile of the water layer adsorbed onto a translucent polymer film could be instantly modulated by 670 nm laser light, applied at an intensity as low as the solar intensity (1000 W m^{-2}) (i.e., the sample was thinner in response to its irradiation). Considering that water is practically transparent to 670 nm light, it was concluded that the resonant laser energy induced fluctuations in the fraction of the water molecules that are partially immobilized in the near-field substrate and thereby ordered.[4] In our earlier experiment, irradiation of the polymer film and simultaneous NSOM were conducted collinearly (normal to the surface of the sample), restricting the approach to translucent samples. The configuration employed here allows us to probe nanoscopic water layers even on samples that are not transparent (e.g., silicon wafers). In particular, the laser irradiation and simultaneous probing of the near-field responses occurred on the same side of the samples—irradiation by a 670 nm laser (power 0.8 mW, local intensity 50 W m^{-2}) and recording resonance spectra via atomic force acoustic microscopy (AFAM).[5] AFAM (Fries Research & Technology, Germany) was carried out under ambient conditions (dim light, temperature 24 °C, relative humidity 61%) by sweeping the frequency in the range of 160 to 230 kHz. It is worth mentioning that with 50 W m^{-2} the applied laser intensity was extremely low: the intensity of a laser pointer of a 1 mW laser (beam $\varnothing \approx 1$ mm) is on the order of 1.3 kW m^{-2}.

Figure 1 shows the basic components of the AFAM experiment and illustrates its principle. The method consists of performing contact mode atomic force microscopy (AFM) on a sample that is mounted on an ultrasonic transducer. Specific contact resonance spectra with typical amplitudes smaller than 1 nm are obtained by recording the vibrational amplitude of the AFM cantilever as a function of the corresponding ultrasonic excitation frequency.

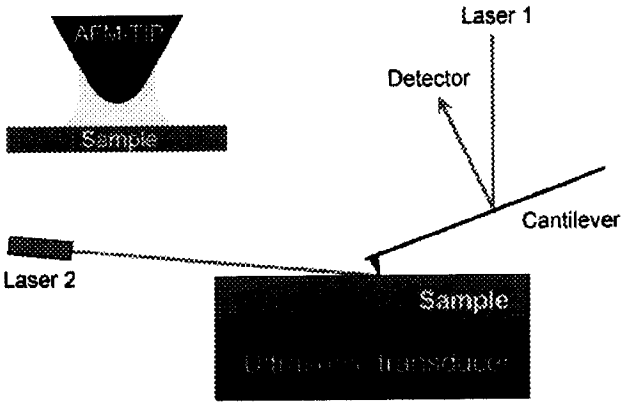

Figure 1. AFAM consists of performing contact mode AFM on an ultrasonically excited sample. The tip−sample interface is irradiated with a 670 nm laser (laser 2) at an angle of incidence of 11.5°. The experimental setup permits the detection of nanoscopic water layers on ultrasmooth substrates. The inset shows the nanoscopic water layer acting as a damping element between the AFM tip and sample.

In the simplest model interpreting the coupling between the AFM tip and sample surface, the tip−sample interaction is described in terms of the classical single spring constant, representing the system's contact stiffness.[6] At moderate oscillations, the resonance curves become symmetric, and changes in the resonance amplitude become manifest. Traditionally, the variation experienced by the oscillating AFM tip is expressed in terms of the quality factor (Q factor), which is inversely proportional to the damping. At resonance, the Q factor is proportional to the vibrational amplitude and can be calculated by dividing the resonance frequency ν_{res} by the half width Δ of the resonance curve: $Q = \nu_{res}/\Delta$. When AFAM is performed at constant resonance frequency and constant excitation amplitude, the resonance amplitude is proportional to the Q factor and inversely proportional to the damping. In general, the resonance amplitude increases with increasing stiffness of the surface.[7] From this perspective, we can expect that nanoscopic water layers adhering to both the sample and tip (hemispherical approximation) and penetrating into the interface (inset of Figure 1) would act

* Corresponding author. E-mail: samoan@gmx.net.
† University of Ulm.
‡ Forschungszentrum Karlsruhe.

(1) Szent-Györgyi, A. *Perspect. Biol. Med.* **1971**, *14*, 239−249.
(2) Sommer, A. P. *J. Phys. Chem. B* **2004**, *108*, 8096−8098.
(3) Sommer, A. P.; Franke, R. P. *Nano Lett.* **2003**, *3*, 19−20.
(4) Sommer, A. P.; Pavlath, A. E. *Cryst. Growth Des.* **2007**, *7*, 18−24.
(5) Rabe, U.; Janser, K.; Arnold, W. *Rev. Sci. Instrum.* **1996**, *67*, 3281−3293.
(6) Hurley, D. C.; Kopycinska-Müller, M.; Kos, A. B.; Geiss, R. H. *Adv. Eng. Mater.* **2005**, *7*, 713−718.
(7) Rabe, U.; Amelio, S.; Kester, E.; Scherer, V.; Hirsekorn, S.; Arnold, W. *Ultrasonics* **2000**, *38*, 430−437.

10.1021/la7032737 CCC: $40.75
Published on Web 01/03/2008

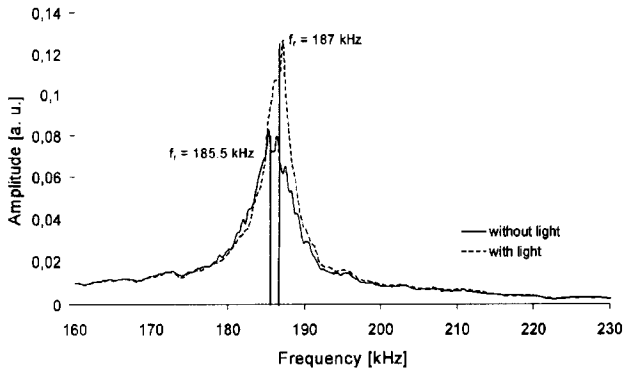

Figure 2. Acoustic atomic force microscopy on polystyrene (hydrophobic), without and with a 670 nm laser. The Q factors for the resonance curves indicate the presence of a water layer between the tip and substrate, which can be tuned by the laser light. The Q factor changed from 26.5 to 39.3, from dim light to laser irradiation, respectively.

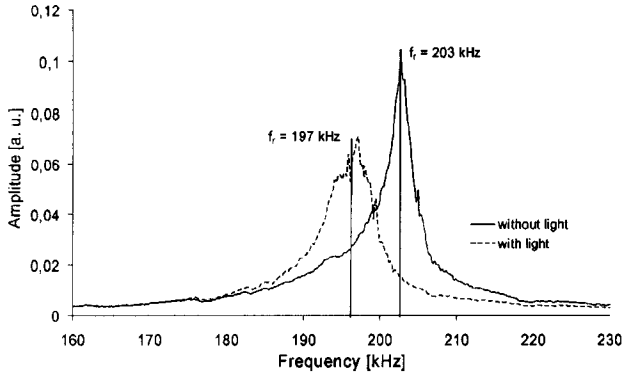

Figure 3. Acoustic atomic force microscopy on silicon (hydrophilic), without and with a 670 nm laser. The Q factors for the resonance curves indicate that there is a more pronounced damping of the tip when the laser is on (cf. Figure 2). The Q factor changed from 34 to 24.5, from dim light to laser irradiation, respectively.

as a damping element operating as a film between the tip and substrate and as a collar around the tip, thereby softening the contact. Consequently, depletion of the damping element would increase the contact stiffness.

Indeed, this is exactly what we observed in the present study. Figure 2 is representative of the resonance behavior on a hydrophobic sample (cover of a polystyrene Petri dish), without and with laser irradiation, confirming our earlier result:[3] $Q_D < Q_L$, where Q_D and Q_L stand for the Q factor without and with laser irradiation of the tip−sample interface, respectively. For the measurements, we used a single-crystal silicon tip mounted on a soft cantilever (0.2 N m^{-1}) and applied a loading force of 5 nN. Next, we investigated the resonance behavior on hydrophilic samples. Interestingly, it was opposite to that found on hydrophobic samples. Figure 3 shows a measurement on a (100) silicone wafer (loading force 10 nN). The Q factors calculated for the resonance curves in Figure 3 indicate that laser irradiation increased the damping in the space between the tip and substrate, expressed in terms of the Q factors: $Q_D > Q_L$.

The increase in damping following laser exposure can be explained on the basis of recent AFM experiments performed in air, which indicated an extremely increased viscosity of interfacial water confined in the space between a hydrophilic tip (Si) and hydrophilic substrates.[8−10] It is probable that this increase (compared to that of bulk water and water layers on hydrophobic surfaces) is simply due to ordered water layers that are thicker on hydrophilic surfaces than on hydrophobic ones.

A qualitative description of viscosity is resistance to flow. Thus, the effect of the applied laser light apparently resulted in a considerable increase in the fluidity of this very viscous water layer, reflected in an increase in damping between the tip and sample, thus facilitating its penetration into the tip−sample interspace. An increase in fluidity is probably equivalent to a decrease in density, where because of the unilateral restriction in mobility the packing density of the molecules constituting the interfacial water layers is probably higher than for those in bulk water. A decrease in density would automatically result in a higher meniscus around the tip, which could explain the increase in damping in response to irradiation. Consistent with the prevalence of thicker water layers on hydrophilic substrates compared to hydrophobic ones, the laser light intensity of 50 W m^{-2} is presumably too small to cause a substantial depletion of the water layers on the silicon wafer. Importantly, the tuning of the water layer was reversible: after switching the laser off, the resonance curve returns to its initial form. And more importantly, the observed shift in amplitude (frequency) disappeared at relative humidity levels of 48% (and below), thus excluding the heating of the AFM tip and/or substrate as the cause of the observed effect. In summary, we established a simple and versatile method based on conventional AFM and an ultrasonic transducer to obtain direct access to the nature of nanoscopic water layers on ultrasmooth substrates. The advantage of the method, whose principle was inspired by the NSOM-based technique introduced by us earlier,[3] is that its applicability is not restricted to translucent substrates. Noting the relevance of nanoscopic water layers as information carriers during cell−cell and cell−biomaterial contacts (first contact events), we expect that the novel method will advance to a central tool in the design of smart biomaterials (i.e., biomaterials with reversibly switchable surface properties[11]). As recently shown, nanoscopic water layers persist in the near-field of solids even in an aqueous environment[4] and therefore have the highest relevance in biological systems. However, in contrast to metallic systems in which the coexistence of an amorphous and a crystalline phase is well characterized[12,13] both theoretically and experimentally, a precise physical picture of the interfacial zone between bulk water and ordered water layers is still lacking, principally because of the indirect nature of the experiments describing this extremely sensitive zone.[4,14] Nevertheless, even without further details it is clear that differently structured nanoscopic water masks on molecules of different polarity are a key element in protein folding (i.e., the hydrophobic effect). Thus, we expect that our results will have a significant impact on life sciences in general and proteomics in particular.

Acknowledgment. We are grateful to the Landesstiftung Baden-Württemberg Bionics Network for financial support. A.P.S. is grateful to Dan Zhu for remembering that there was an intense thunderstorm over Ulm on the day of the first successful AFAM measurement (which was responsible for a relative humidity value of 61% in the laboratory and key to the reproducibility of the experiment).

LA7032737

(8) Goertz, M. P.; Houston, J. E.; Zhu, X. Y. *Langmuir* **2007**, *23*, 5491−5497.
(9) Jinesh, K. B.; Frenken, J. W. M. *Phys. Rev. Lett.* **2006**, *96*, 166103.
(10) Li, T. D.; Gao, J.; Szoszkiewicz, R.; Landman, U.; Riedo, E. *Phys. Rev. B* **2007**, *75*, 115415.
(11) Lahann, J.; Mitragotri, S.; Tran, T. N.; Kaido, H.; Sundaram, J.; Choi, I. S.; Hoffer, S.; Somorjai, G. A.; Langer, R. *Science* **2003**, *299*, 371−374.
(12) Fecht, H. J. *Nature* **1992**, *356*, 133−135.
(13) Lojkowski, W.; Fecht, H. J. *Prog. Mater. Sci.* **2000**, *45*, 339−568.
(14) Sommer, A. P.; Zhu, D.; Brühne, K. *Cryst. Growth Des.* **2007**, *7*, 2298−2301.

EXHIBIT 5

POTASSIUM CHANNELS AND THE ATOMIC BASIS OF SELECTIVE ION CONDUCTION

Nobel Lecture, December 8, 2003

by

RODERICK MACKINNON

Howard Hughes Medical Institute, Laboratory of Molecular Neurobiology and Biophysics, Rockefeller University, 1230 York Avenue, New York, NY 10021, USA.

INTRODUCTION

All living cells are surrounded by a thin, approximately 40 Å thick lipid bilayer called the cell membrane. The cell membrane holds the contents of a cell in one place so that the chemistry of life can occur, but it is a barrier to the movement of certain essential ingredients including the ions Na^+, K^+, Ca^{2+} and Cl^-. The barrier to ion flow across the membrane – known as the dielectric barrier – can be understood at an intuitive level: the cell membrane interior is an oily substance and ions are more stable in water than in oil. The energetic preference of an ion for water arises from the electric field around the ion and its interaction with neighboring molecules. Water is an electrically polarizable substance, which means that its molecules rearrange in an ion's electric field, pointing negative oxygen atoms in the direction of cations and positive hydrogen atoms toward anions. These electrically stabilizing interactions are much weaker in a less polarizable substance such as oil. Thus, an ion will tend to stay in the water on either side of a cell membrane rather than enter and cross the membrane. And yet numerous cellular processes, ranging from electrolyte transport across epithelia to electrical signal production in neurons, depend on the flow of ions across the membrane. To mediate the flow, specific protein catalysts known as ion channels exist in the cell membrane. Ion channels exhibit the following three essential properties: (1) they conduct ions rapidly, (2) many ion channels are highly selective, meaning only certain ion species flow while others are excluded, (3) their function is regulated by processes known as gating, that is, ion conduction is turned on and off in response to specific environmental stimuli. Figure 1 summarizes these properties (figure 1).

The modern history of ion channels began in 1952 when Hodgkin and Huxley published their seminal papers on the theory of the action potential in the squid giant axon (Hodgkin and Huxley, 1952a; Hodgkin and Huxley, 1952b; Hodgkin and Huxley, 1952c; Hodgkin and Huxley, 1952d). A fundamental element of their theory was that the axon membrane undergoes changes in its permeability to Na^+ and K^+ ions. The Hodgkin-Huxley theory

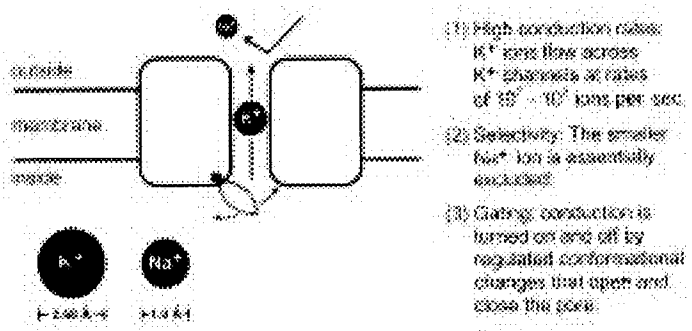

Figure 1. Ion channels exhibit three basic properties depicted in the cartoon. They conduct specific ions (for example K^+) at high rates, they are selective (a K^+ channel essentially excludes Na^+), and conduction is turned on and off by opening and closing a gate, which can be regulated by an external stimulus such as ligand-binding or membrane voltage. The relative size of K^+ and Na^+ ions is shown.

did not address the mechanism by which the membrane permeability changes occur: ions could potentially cross the membrane through channels or by a carrier-mediated mechanism. In their words 'Details of the mechanism will probably not be settled for some time' (Hodgkin and Huxley, 1952a). It is fair to say that the pursuit of this statement has accounted for much ion channel research over the past fifty years.

As early as 1955 experimental evidence for channel mediated ion flow was obtained when Hodgkin and Keynes measured the directional flow of K^+ ions across axon membranes using the isotope $^{42}K^+$ (Hodgkin and Keynes, 1955). They observed that K^+ flow in one direction across the membrane depends on flow in the opposite direction, and suggested that 'the ions should be constrained to move in single file and that there should, on average, be several ions in a channel at any moment'. Over the following two decades Armstrong and Hille used electrophysiological methods to demonstrate that Na^+ and K^+ ions cross cell membranes through unique protein pores – Na^+ channels and K^+ channels – and developed the concepts of selectivity filter for ion discrimination and gate for regulating ion flow (Hille, 1970; Hille, 1971; Hille, 1973; Armstrong, 1971; Armstrong *et al.*, 1973; Armstrong and Bezanilla, 1977; Armstrong, 1981). The patch recording technique invented by Neher and Sakmann then revealed the electrical signals from individual ion channels, as well as the extraordinary diversity of ion channels in living cells throughout nature (Neher and Sakmann, 1976).

The past twenty years have been the era of molecular biology for ion channels. The ability to manipulate amino acid sequences and express ion channels at high levels opened up entirely new possibilities for analysis. The advancement of techniques for protein structure determination and the development of synchrotron facilities also created new possibilities. For me, a scientist who became fascinated with understanding the atomic basis of life's electrical system, there could not have been a more opportune time to enter the field.

MY EARLY STUDIES: THE K^+ CHANNEL SIGNATURE SEQUENCE

The cloning of the *Shaker* K^+ channel gene from *Drosophila melanogaster* by Jan, Tanouye, and Pongs revealed for the first time a K^+ channel amino acid sequence and stimulated efforts by many laboratories to discover which of these amino acids form the pore, selectivity filter, and gate (Tempel *et al.*, 1987; Kamb *et al.*, 1987; Pongs *et al.*, 1988). At Brandeis University in Chris Miller's laboratory I had an approach to find the pore amino acids. Chris and I had just completed a study showing that charybdotoxin, a small protein from scorpion venom, inhibits a K^+ channel isolated from skeletal muscle cells by plugging the pore and obstructing the flow of ions (MacKinnon and Miller, 1988). In one of those late night 'let's see what happens if' experiments while taking a molecular biology course at Cold Spring Harbor I found that the toxin – or what turned out to be a variant of it present in the charybdotoxin preparation – inhibited the Shaker K^+ channel (MacKinnon *et al.*, 1988; Garcia *et al.*, 1994). This observation meant I could use the toxin to find the pore, and it did not take very long to identify the first site-directed mutants of the Shaker K^+ channel with altered binding of toxin (MacKinnon and Miller, 1989). I continued these experiments at Harvard Medical School where I began as assistant professor in 1989. Working with my small group at Harvard, including Tatiana Abramson, Lise Heginbotham, and Zhe Lu, and sometimes with Gary Yellen at Johns Hopkins University, we reached several interesting conclu-

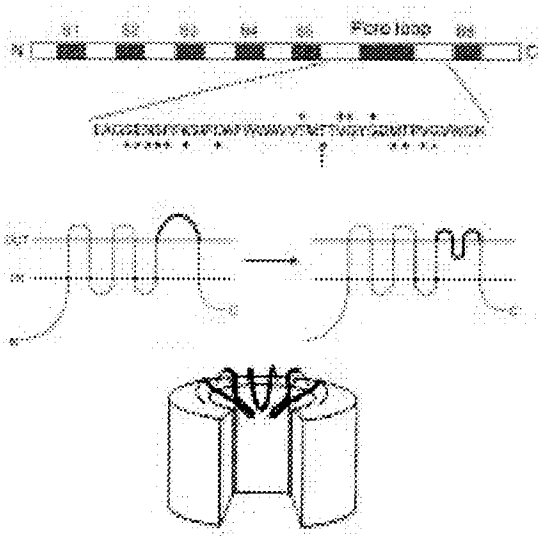

Figure 2. Early picture of a tetramer K^+ channel with a selectivity filter made of pore loops. A linear representation of a Shaker K^+ channel subunit on top shows shaded hydrophobic segments S1 to S6 and a region designated the pore loop. A partial amino acid sequence from the Shaker K^+ channel pore loop highlights amino acids shown to interact with extracellular scorpion toxins (*), intracellular tetraethylammonium (↑) and K^+ ions (+). The pore loop was proposed to reach into the membrane (middle) and form a selectivity filter at the center of four subunits (bottom).

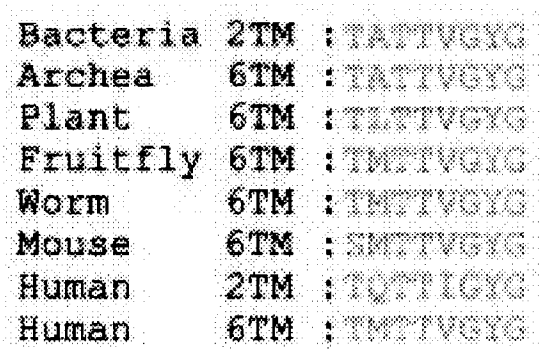

Figure 3. The K^+ channel signature sequence shown as single letter amino acid code (blue) is highly conserved in organisms throughout the tree of life. Some K^+ channels contain six membrane-spanning segments per subunit (6TM) while others contain only two (2TM). 2TM K^+ channels correspond to 6TM K^+ channels without the first four membrane-spanning segments (S1-S4 in figure 2).

sions concerning the architecture of K^+ channels. They had to be tetramers in which four subunits encircle a central ion pathway (MacKinnon, 1991). This conclusion was not terribly surprising but the experiments and analysis to reach it gave me great pleasure since they required only simple measurements and clear reasoning with binomial statistics. We also deduced that each subunit presents a 'pore loop' to the central ion pathway (figure 2) (MacKinnon, 1995). This 'loop' formed the binding sites for scorpion toxins (MacKinnon and Miller, 1989; Hidalgo and MacKinnon, 1995; Ranganathan *et al.*, 1996) as well as the small-molecule inhibitor tetraethylammonium ion (MacKinnon and Yellen, 1990; Yellen *et al.*, 1991), which had been used by Armstrong and Hille decades earlier in their pioneering analysis of K^+ channels (Armstrong, 1971; Armstrong and Hille, 1972). Most important to my thinking, mutations of certain amino acids within the 'loop' affected the channel's ability to discriminate between K^+ and Na^+, the selectivity hallmark of K^+ channels (Heginbotham *et al.*, 1992; Heginbotham *et al.*, 1994). Meanwhile, new K^+ channel genes were discovered and they all had one obvious feature in common: the very amino acids that we had found to be important for K^+ selectivity were conserved (figure 3). We called these amino acids the K^+ channel signature sequence, and imagined four pore loops somehow forming a selectivity filter with the signature sequence amino acids inside the pore (Heginbotham *et al.*, 1994; MacKinnon, 1995).

When you consider the single channel conductance of many K^+ channels found in cells you realize just how incredible these molecular devices are. With typical cellular electrochemical gradients, K^+ ions conduct at a rate of 10^7 to 10^8 ions per second. That rate approaches the expected collision frequency of K^+ ions from solution with the entryway to the pore. This means that K^+ ions flow through the pore almost as fast as they diffuse up to it. For this to occur the energetic barriers in the channel have to be very low, something like those encountered by K^+ ions diffusing through water. All the more

remarkable, the high rates are achieved in the setting of exquisite selectivity: the K^+ channel conducts K^+, a monovalent cation of Pauling radius 1.33 Å, while essentially excluding Na^+, a monovalent cation of Pauling radius 0.95 Å. And this ion selectivity is critical to the survival of a cell. How does nature accomplish high conduction rates and high selectivity at the same time? The answer to this question would require knowing the atomic structure formed by the signature sequence amino acids, that much was clear. The conservation of the signature sequence amino acids in K^+ channels throughout the tree of life, from bacteria (Milkman, 1994) to higher eukaryotic cells, implied that nature had settled upon a very special solution to achieve rapid, selective K^+ conduction across the cell membrane. For me, this realization provided inspiration to want to directly visualize a K^+ channel and its selectivity filter.

THE KCSA STRUCTURE AND SELECTIVE K^+ CONDUCTION

I began to study crystallography, and although I had no idea how I would obtain funding for this endeavor, I have always believed that if you really want to do something then you will find a way. By happenstance I explained my plan to Torsten Wiesel, then president of Rockefeller University. He suggested that I come to Rockefeller where I would be able to concentrate on the problem. I accepted his offer and moved there in 1996. In the beginning I was joined by Declan Doyle and my wife Alice Lee MacKinnon and within a year others joined including João Morais Cabral, John Imredy, Sabine Mann and Richard Pfuetzner. We had to learn as we went along, and what we may have lacked in size and skill we more than compensated for with enthusiasm. It was a very special time. At first I did not know how we would ever reach the point of obtaining enough K^+ channel protein to attempt crystallization, but the K^+ channel signature sequence continued to appear in a growing number of prokaryotic genes, making expression in *Escherichia coli* possible. We focused our effort on a bacterial K^+ channel called KcsA from *Streptomyces lividans*, discovered by Schrempf (Schrempf *et al.*, 1995). The KcsA channel has a simple topology with only two membrane spanning segments per subunit corresponding to the Shaker K^+ channel without S1 through S4 (figure 2). Despite its prokaryotic origin KcsA closely resembled the Shaker K^+ channel's pore amino acid sequence, and even exhibited many of its pharmacological properties, including inhibition by scorpion toxins (MacKinnon *et al.*, 1998). This surprised us from an evolutionary standpoint, because why should a scorpion want to inhibit a bacterial K^+ channel! But from the utilitarian point of view of protein biophysicists we knew exactly what the scorpion toxin sensitivity meant, that KcsA had to be very similar in structure to the Shaker K^+ channel.

The KcsA channel produced crystals but they were poorly ordered and not very useful in the X-ray beam. After we struggled for quite a while I began to wonder whether some part of the channel was intrinsically disordered and interfering with crystallization. Fortunately my neighbor Brian Chait and his postdoctoral colleague Steve Cohen were experts in the analysis of soluble proteins by limited proteolysis and mass spectrometry, and their techniques

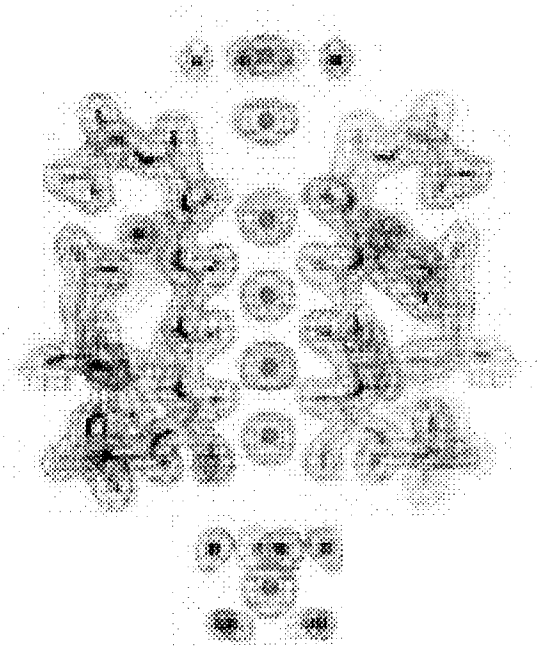

Figure 4. Electron density ($2F_o$-F_c contoured at 2 σ) from a high-resolution structure of the KcsA K^+ channel is shown as blue mesh. This region of the channel features the selectivity filter with K^+ ions and water molecules along the ion pathway. The refined atomic model is shown in the electron density. Adapted from (Zhou *et al.*, 2001b).

applied beautifully to a membrane protein. We found that KcsA was as solid as a rock, except for its C-terminus. After removing disordered amino acids from the c-terminus with chymotrypsin the crystals improved dramatically, and we were able to solve an initial structure at a resolution of 3.2 Å (Doyle *et al.*, 1998). We could not clearly see K^+ in the pore at this resolution, but my years of work on K^+ channel function told me that Rb^+ and Cs^+ should be valuable electron dense substitutes for K^+, and they were. Rubidium and Cs^+ difference Fourier maps showed these ions lined up in the pore – as Hodgkin and Keynes might have imagined in 1955 (Hodgkin and Keynes, 1955).

The KcsA structure was altogether illuminating, but before I describe it, I will depart from chronology to explain the next important technical step. A very accurate description of the ion coordination chemistry inside the selectivity filter would require a higher resolution structure. With 3.2 Å data we could infer the positions of the main-chain carbonyl oxygen atoms by applying our knowledge of small molecule structures, that is our chemical intuition, but we needed to see the selectivity filter atoms in detail. A high-resolution structure was actually quite difficult to obtain. After more than three additional years of work by João and then Yufeng (Fenny) Zhou we finally managed to produce high-quality crystals by attaching monoclonal Fab fragments to KcsA. These crystals provided the information we needed, a structure at a resolution of 2.0 Å in which K^+ ions could be visualized in the grasp of selec-

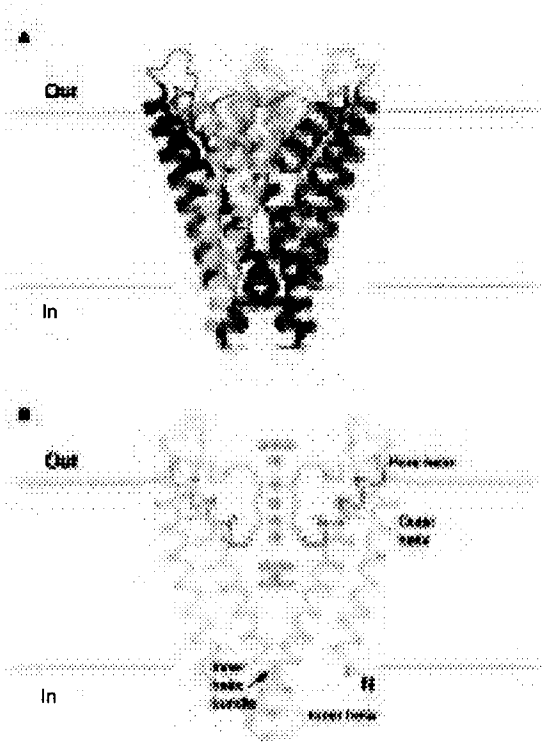

Figure 5. (A) A ribbon representation of the KcsA K^+ channel with its four subunits colored uniquely. The channel is oriented with the extracellular solution on top. (B) The KcsA K^+ channel with front and back subunits removed, colored to highlight the pore-helices (red) and selectivity filter (yellow). Electron density in blue mesh is shown along the ion pathway. Labels identify the pore, outer, and inner helices and the inner helix bundle. The outer and inner helices correspond to S5 and S6 in figure 2.

tivity filter protein atoms (figure 4) (Zhou *et al.*, 2001b). What did the K^+ channel structure tell us and why did nature conserve the K^+ channel signature sequence amino acids?

Not all protein structures speak to you in an understandable language, but the KcsA K^+ channel does. Four subunits surround a central ion pathway that crosses the membrane (figure 5A). Two of the four subunits are shown in figure 5B with electron density from K^+ ions and water along the pore. Near the center of the membrane the ion pathway is very wide, forming a cavity about 10 Å in diameter with a hydrated K^+ ion at its center. Each subunit directs the C-terminal end of a 'pore helix', shown in red, toward the ion. The C-terminal end of an α-helix is associated with a negative 'end charge' due to carbonyl oxygen atoms that do not participate in secondary structure hydrogen bonding, so the pore helices are directed as if to stabilize the K^+ ion in the cavity. At the beginning of this lecture I raised the fundamental issue of the cell membrane being an energetic barrier to ion flow because of its oily interior. KcsA allows us to intuit a simple logic encoded in its structure, and electrostatic calculations support the intuition (Roux and MacKinnon, 1999): the K^+ channel lowers the membrane dielectric barrier by hydrating a K^+ ion deep inside the membrane, and by stabilizing it with α-helix end charges.

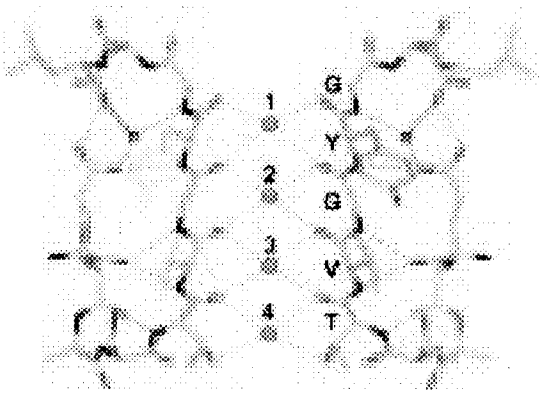

Figure 6. Detailed structure of the K^+ selectivity filter (two subunits). Oxygen atoms coordinate K^+ ions (green spheres) at positions 1 to 4 from the extracellular side. Single letter amino acid code identifies select signature sequence amino acids. Yellow, blue and red correspond to carbon, nitrogen and oxygen atoms, respectively. Green and gray dashed lines show oxygen-K^+ and hydrogen bonding interactions.

How does the K^+ channel distinguish K^+ from Na^+? Our earlier mutagenesis studies had indicated that the signature sequence amino acids would be responsible for this most basic function of a K^+ channel. Figure 6 shows the structure formed by the signature sequence – the selectivity filter – located in the extracellular third of the ion pathway. The glycine amino acids in the sequence TVGYG have dihedral angles in or near the left-handed helical region of the Ramachandran plot, as does the threonine, allowing the main-chain carbonyl oxygen atoms to point in one direction, toward the ions along the pore. It is easy to understand why this sequence is so conserved among K^+ channels: the alternating glycine amino acids permit the required dihedral angles, the threonine hydroxyl oxygen atom coordinates a K^+ ion, and the side-chains of valine and tyrosine are directed into the protein core surrounding the filter to impose geometric constraint. The end result when the subunits come together is a narrow tube consisting of four equal spaced K^+ binding sites, labeled 1 to 4 from the extracellular side. Each binding site is a cage formed by eight oxygen atoms on the vertices of a cube, or a twisted cube called a square antiprism (figure 7). The binding sites are very similar to the single alkali metal site in nonactin, a K^+ selective antibiotic with nearly identical K^+-oxygen distances (Dobler *et al.*, 1969; Dunitz and Dobler, 1977). The principle of K^+ selectivity is implied in a subtle feature of the KcsA crystal structure. The oxygen atoms surrounding K^+ ions in the selectivity filter are arranged quite like the water molecules surrounding the hydrated K^+ ion in the cavity. This comparison conveys a visual impression of binding sites in the filter paying for the energetic cost of K^+ dehydration. The Na^+ ion is apparently too small for these K^+-sized binding sites, so its dehydration energy is not compensated.

The question that compelled us most after seeing the structure was exactly

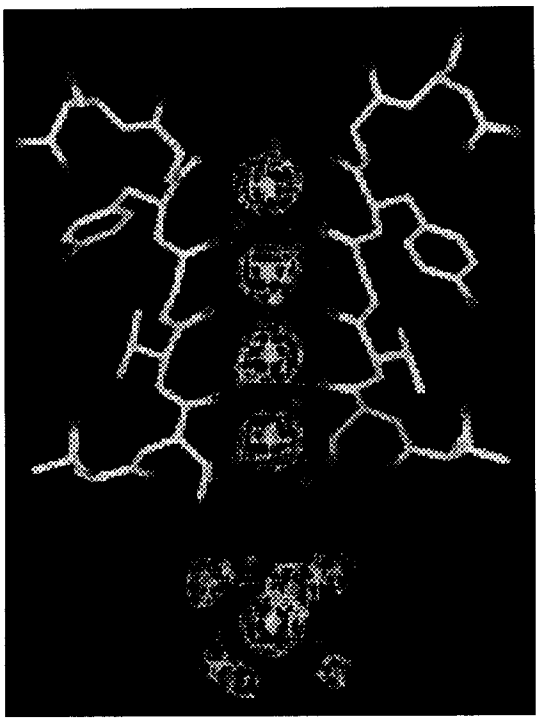

Figure 7. A K^+ channel mimics the hydration shell surrounding a K^+ ion. Electron density (blue mesh) for K^+ ions in the filter and for a K^+ ion and water molecules in the central cavity are shown. White lines highlight the coordination geometry of K^+ in the filter and in water. Adapted from (Zhou *et al.*, 2001b).

how many ions are in the selectivity filter at a given time? To begin to understand how ions move through the filter we needed to know the stoichiometry of the ion conduction reaction, and that meant knowing how many ions can occupy the filter. Four binding sites were apparent, but are they all occupied at once? Four K^+ ions in a row separated by an average center-to-center distance of 3.3 Å seemed unlikely for electrostatic reasons. From an early stage we suspected that the correct number would be closer to two, because two ions more easily explained the electron density we observed for the larger alkali metal cations Rb^+ and Cs^+ (Doyle *et al.*, 1998; Morais-Cabral *et al.*, 2001). Quantitative evidence for the precise number of ions came with the high-resolution structure and with the analysis of Tl^+ (Zhou and MacKinnon, 2003). Thallium is the most ideally suited 'K^+ analog' because it flows through K^+ channels, has a radius and dehydration energy very close to K^+, and has the favorable crystallographic attributes of high electron density and an anomalous signal. The one serious difficulty in working with Tl^+ is its insolubility with Cl^-. Fenny meticulously worked out the experimental conditions and determined that on average there are between two and two and a half conducting ions in the filter at once, with an occupancy at each position around one half.

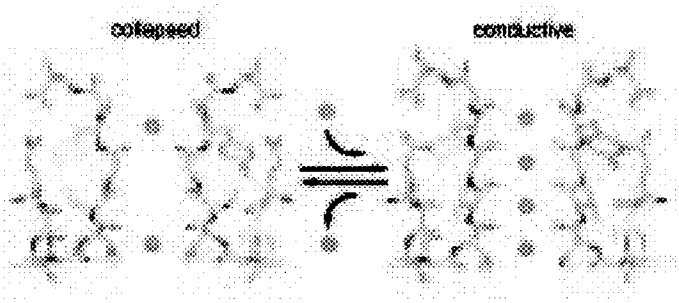

Figure 8. The selectivity filter can adopt two conformations. At low concentrations of K^+ on average one K^+ ion resides at either of two sites near the ends of the filter, which is collapsed in the middle. At high concentrations of K^+ a second ion enters the filter as it changes to a conductive conformation. On average, two K^+ ions in the conductive filter reside at four sites, each with about half occupancy.

We also observed that if the concentration of K^+ (or Tl^+) bathing the crystals is lowered sufficiently (below normal intracellular levels) then a reduction in the number of ions from two to one occurs and is associated with a structural change to a 'collapsed' filter conformation, which is pinched closed in the middle (Zhou *et al.*, 2001b; Zhou and MacKinnon, 2003). At concentrations above 20 mM the entry of a second K^+ ion drives the filter to a 'conductive' conformation, as shown in figure 8. Sodium on the other hand does not drive the filter to a 'conductive' conformation even at concentrations up to 500 mM.

The K^+-induced conformational change has thermodynamic consequences for the affinity of two K^+ ions in the 'conductive' filter. It implies that a fraction of the second ion's binding energy must be expended as work to bring about the filter's conformational change, and as a result the two ions will bind with reduced affinity. To understand this statement at an intuitive level, recognize that for two ions to reside in the filter they must oppose its tendency to collapse and force one of them out, i.e. the two-ion 'conductive' conformation is under some tension, which will tend to lower K^+ affinity. This is a desirable property for an ion channel because weak binding favors high conduction rates. The same principle, referred to as the 'induced fit' hypothesis, had been proposed decades earlier by enzymologists to explain high specificity with low substrate affinity in enzyme catalysis (Jencks, 1987).

In the 'conductive' filter if two K^+ ions were randomly distributed then they would occupy four sites in six possible ways. But several lines of evidence hinted to us that the ion positions are not random. For example Rb^+ and Cs^+ exhibit preferred positions with obviously low occupancy at position 2 (Morais-Cabral *et al.*, 2001; Zhou and MacKinnon, 2003). In K^+ we observed an unusual doublet peak of electron density at the extracellular entryway to the selectivity filter, shown in figure 9 (Zhou *et al.*, 2001b). We could explain this density if K^+ is attracted from solution by the negative protein surface charge near the entryway and at the same time repelled by K^+ ions inside the filter. Two discrete peaks implied two distributions of ions in the filter. If K^+ ions

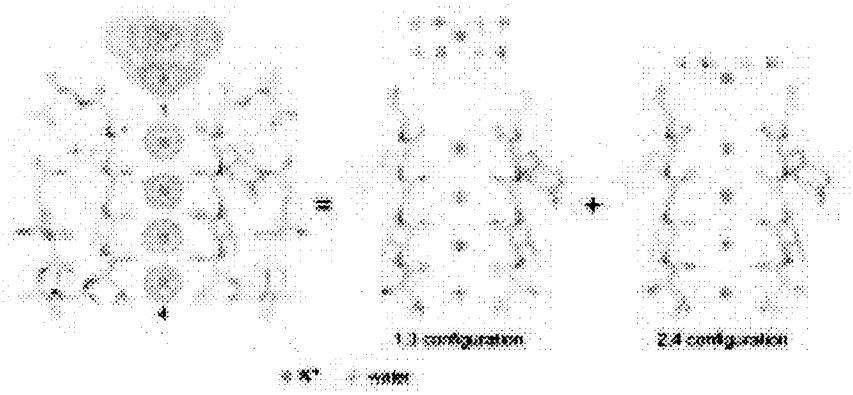

Figure 9. Two K^+ ions in the selectivity filter are hypothesized to exist predominantly in two specific configurations 1,3 and 2,4 as shown. K^+ ions and water molecules are shown as green and red spheres, respectively. Adapted from (Zhou *et al.*, 2001b).

tend to be separated by a water molecule for electrostatic reasons then the two dominant configurations would be 1,3 (K^+ ions in positions 1 and 3 with a water molecule in between) and 2,4 (K^+ ions in positions 2 and 4 with a water molecule in between). A mutation at position 4 (threonine to cysteine) was recently shown to influence K^+ occupancy at positions 2 and 4 but not at 1 and 3, providing strong evidence for specific 1,3 and 2,4 configurations of K^+ ions inside the selectivity filter (Zhou and MacKinnon, 2004).

Discrete configurations of an ion pair suggested a mechanism for ion conduction (figure 10A) (Morais-Cabral *et al.*, 2001). The K^+ ion pair could diffuse back and forth between 1,3 and 2,4 configurations (bottom pathway), or alternatively an ion could enter the filter from one side of the membrane as the ion-water queue moves and a K^+ exits at the opposite side (the top pathway). Movements would have to be concerted because the filter is no wider than a K^+ ion or water molecule. The two paths complete a cycle: in one complete cycle each ion moves only a fraction of the total distance through the filter, but the overall electrical effect is to move one charge all the way. Because two K^+ ions are present in the filter throughout the cycle we expect there should be electrostatic repulsion between them. Together with the filter conformational change that is required to achieve a 'conductive' filter with two K^+ ions in it, electrostatic repulsion should favor high conduction rates by lowering K^+ affinity.

Absolute rates from 10^7 to 10^8 ions per second are truly impressive for a highly selective ion channel. One aspect of the crystallographic data suggests that very high conductance K^+ channels such as KcsA might operate near the maximum rate that the conduction mechanism will allow. All four positions in the filter have a K^+ occupancy close to one half, which implies that the 1,3 and 2,4 configurations are equally probable, or energetically equivalent, but there is no *a priori* reason why this should be. A simulation of ions diffusing around the cycle offers a possible explanation: maximum flux is achieved when the energy difference between the 1,3 and 2,4 configurations is zero be-

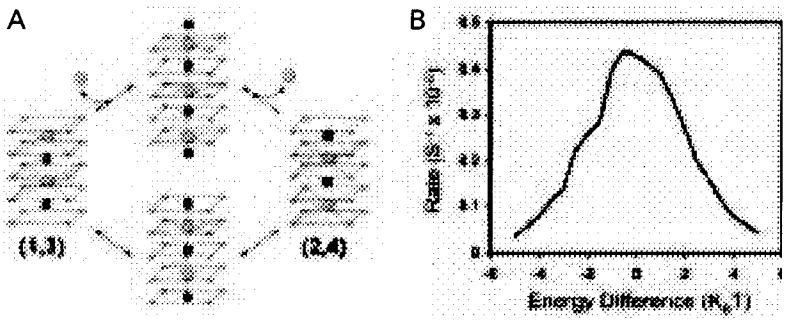

Figure 10. (A) Through-put cycle for K^+ conduction invoking 1,3 and 2,4 configurations. The selectivity filter is represented as five square planes of oxygen atoms. K^+ and water are shown as green and red spheres, respectively. (B) Simulated K^+ flux around the cycle is graphed as a function of the energy difference between the 1,3 and 2,4 configurations. Adapted from (Morais-Cabral *et al.*, 2001).

cause that is the condition under which the 'energy landscape' for the conduction cycle is smoothest (figure 10B). The energetic balance between the configurations therefore might reflect the optimization of conduction rate by natural selection (Morais-Cabral *et al.*, 2001). It is not so easy to demonstrate this point experimentally but it is certainly fascinating to ponder.

COMMON STRUCTURAL PRINCIPLES UNDERLIE K^+ AND Cl^- SELECTIVITY

The focus of this lecture is K^+ channels, but for a brief interlude I would like to show you a Cl^- selective transport protein. By comparing a K^+ channel and a Cl^- 'channel' we can begin to appreciate familiar themes in nature's solutions to different problems: getting cations and anions across the cell membrane. ClC Cl^- channels are found in many different cell types and are associated with a number of physiological processes that require Cl^- ion flow across lipid membranes (Jentsch *et al.*, 1999; Maduke *et al.*, 2000). As is the case for K^+ channels, ClC family genes are abundant in prokaryotes, a fortunate circumstance for protein expression and structural analysis. When Raimund Dutzler joined my laboratory he, Ernest Campbell and I set out to address the structural basis of Cl^- ion selectivity. We determined crystal structures of two bacterial members of the ClC Cl^- channel family, one from *Escherichia coli* (EcClC) and another from *Salmonella typhimurium* (StClC) (Dutzler *et al.*, 2002). Recent studies by Miller on the function of EcClC have shown that it is actually a Cl^- – proton exchanger (Accardi and Miller, 2004). We do not yet know why certain members of this family of Cl^- transport proteins function as channels and others as exchangers, but the crystal structures are fascinating and give us a view of Cl^- selectivity. Architecturally the ClC proteins are unrelated to K^+ channels, but if we focus on the ion pathway certain features are similar (figure 11). As we saw in K^+ channels, the ClC proteins have α-helices pointed at the ion pathway, but the direction is reversed with the positive

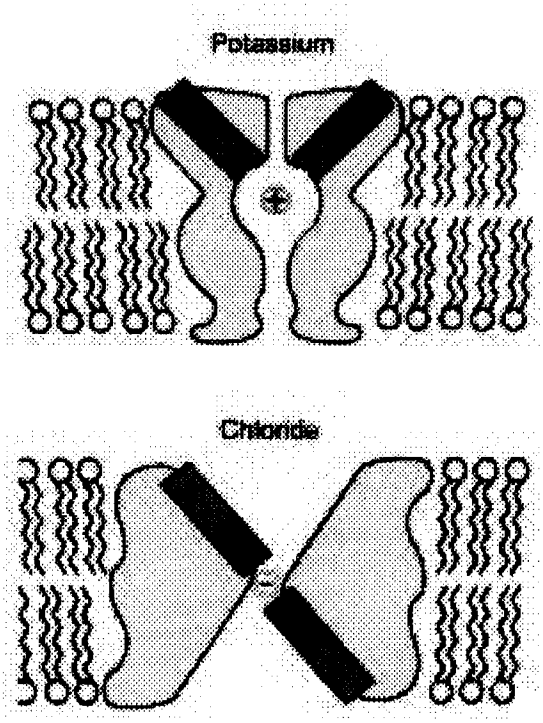

Figure 11. The overall architecture of K^+ channels and ClC Cl^- transport proteins is very different but certain general features are similar. One similarity shown here is the use of α-helix end charges directed toward the ion pathway. The negative C-terminal end charge (red) points to K^+. The positive N-terminal end charge (blue) points to Cl^-.

charge of the N-terminus close to Cl^-. This makes perfect sense for lowering the dielectric barrier for a Cl^- ion. In ClC we see that ions in its selectivity filter tend to be coordinated by main chain protein atoms, with amide nitrogen atoms surrounding Cl^- instead of carbonyl oxygen atoms surrounding K^+ (figure 12). We also see that both the K^+ and Cl^- selectivity filters contain multiple close-spaced binding sites and appear to contain more than one ion, perhaps to exploit electrostatic repulsion between ions in the pore. I find these similarities fascinating. They tell us that certain basic physical principles are important, such as the use of α-helix end charges to lower the dielectric barrier when ions cross the lipid membrane.

TRYING TO SEE A K^+ CHANNEL OPEN AND CLOSE

Most ion channels conduct when called upon by a specific stimulus such as the binding of a ligand or a change in membrane voltage (Hille, 2001). The processes by which ion conduction is turned on are called gating. The conduction of ions occurs on a time scale that is far too rapid to involve very large protein conformational changes. That is undoubtedly one of the reasons why a single KcsA structure could tell us so much about ion selectivity and con-

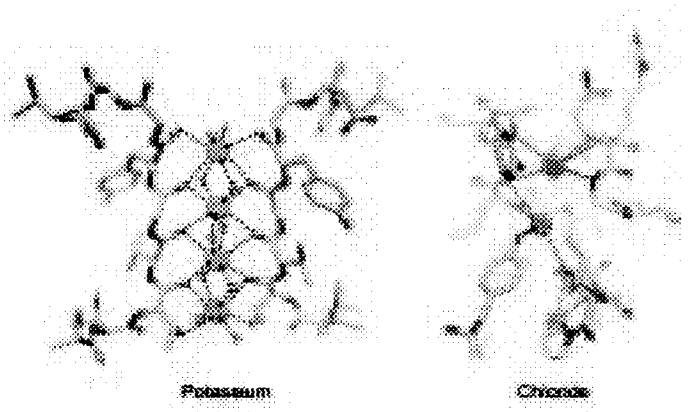

Figure 12. K^+ and Cl^- selectivity filters make use of main chain atoms to coordinate ions: carbonyl oxygen atoms for K^+ ions (green spheres) and amide nitrogen atoms for Cl^- ions (red spheres). Both filters contain multiple close-spaced ion binding sites. The Cl^- selectivity filter is that of a mutant ClC in which a glutamate amino acid was changed to glutamine (Dutzler *et al.*, 2003).

duction. Gating on the other hand occurs on a much slower time scale and can involve large protein conformational changes. The challenge for a structural description of gating is to capture a channel in both opened (on) and closed (off) conformations so that they can be compared.

In the KcsA K^+ channel gating is controlled by intracellular pH and lipid membrane composition, but unfortunately the KcsA channel's open probability reaches a maximum value of only a few percent in functional assays (Cuello *et al.*, 1998; Heginbotham *et al.*, 1998). At first we had no definitive way to know whether a gate was open or closed in the crystal structures. In the 1970s Armstrong had proposed the existence of a gate near the intracellular side of the membrane in voltage dependent K^+ channels because he could 'trap' large organic cations inside the pore between a selectivity filter near the extracellular side and a gate near the intracellular side (Armstrong, 1971; Armstrong, 1974). Following these ideas we crystallized KcsA with a heavy atom version of one of his organic cations, tetrabutyl antimony (TBA), and found that it binds inside the central cavity of KcsA (Zhou *et al.*, 2001a). This was very interesting because the ~10 Å diameter of TBA far exceeds the pore diameter leading up to the cavity: in KcsA the intracellular pore entryway is constricted to about 3.5 Å by the inner helix bundle (figure 5B). Seeing TBA 'trapped' in the cavity behind the inner helix bundle evoked Armstrong's classical view of K^+ channel gating, and implied that the inner helix bundle serves as a gate and is closed in KcsA. Mutational and spectroscopic studies in other laboratories also pointed to the inner helix bundle as a possible gate-forming structural element (Perozo *et al.*, 1999; del Camino *et al.*, 2000).

Youxing Jiang and I hoped we could learn more about K^+ channel gating by determining the structures of new K^+ channels. From gene sequence analysis we noticed that many prokaryotic K^+ channels contain a large C-ter-

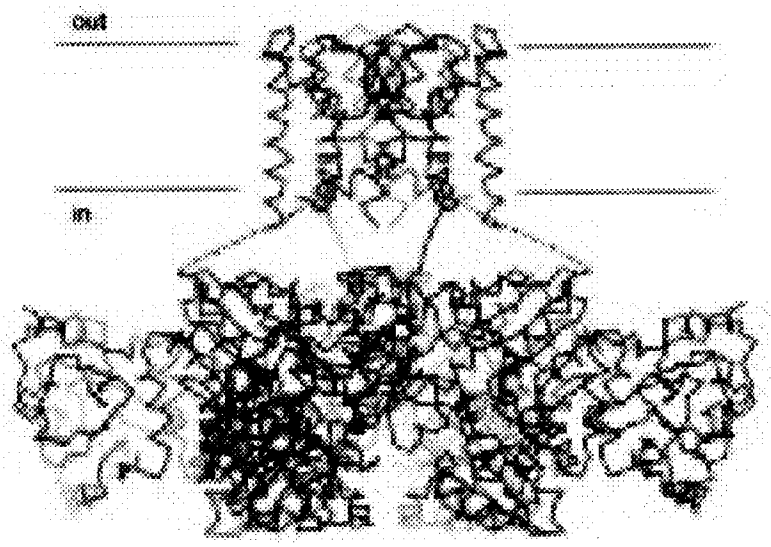

Figure 13. The MthK K^+ channel contains an intracellular gating ring (bottom) attached to its ion conduction pore (top). Ca^{2+} ions (yellow spheres) are bound to the gating ring in clefts in between domains. The connections between the gating ring and the pore, which were poorly ordered in the crystal, are shown as dashed lines.

minus that encodes what we called RCK domains and we suspected that these domains control pore opening, perhaps through binding of an ion or a small-molecule. Initally we determined the structure of isolated RCK domains from an *Escherichia coli* K^+ channel, but by themselves they were not very informative beyond hinting that a similar structure exists on the C-terminus of eukaryotic Ca^{2+}-dependent 'BK' channels (Jiang *et al.*, 2001). We subsequently determined the crystal structure of MthK, complete K^+ channel containing RCK domains, from *Methanobacterium thermoautotrophicus* (figure 13) (Jiang *et al.*, 2002a). This structure was extremely informative. The RCK domains form a 'gating ring' on the intracellular side of the pore. In clefts between domains we could see what appeared to be divalent cation binding sites, and the crystals had been grown in the presence of Ca^{2+}. In functional assays we discovered that the open probability of the MthK channel increased as Ca^{2+} or Mg^{2+} concentration was raised, giving us good reason to believe that the crystal structure should represent the open conformation of a K^+ channel.

In our MthK structure the inner helix bundle is opened like the aperture of a camera (figure 14) (Jiang *et al.*, 2002b). As a result, the pathway leading up to the selectivity filter from the intracellular side is about 10 Å wide, explaining how Armstrong's large organic cations can enter the cavity to block a K^+ channel, and how K^+ ions gain free access to the selectivity filter through aqueous diffusion. By comparing the KcsA and MthK channel structures it seemed that we were looking at examples of closed and opened K^+ channels, and could easily imagine the pore undergoing a conformational change from closed to open. To open, the inner helices would have to bend at a point halfway across

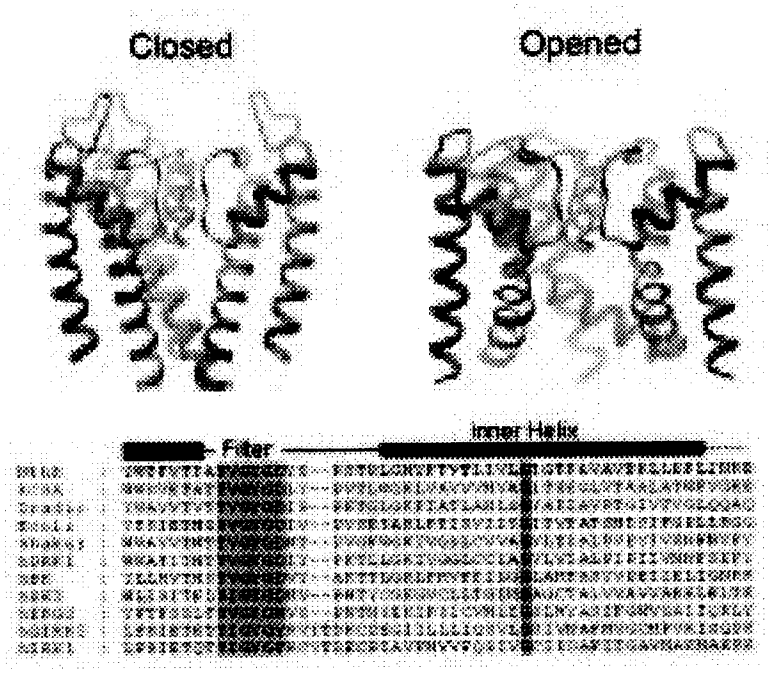

Figure 14. KcsA and MthK represent closed and opened K^+ channels. Three subunits of the closed KcsA K^+ channel (left) and opened MthK K^+ channel (right) are shown. The inner helices of MthK are bent at a glycine gating hinge (red), allowing the inner helix bundle to open. Partial amino acid sequences from a variety of K^+ channels with different gating domains are compared. Colors highlighting the selectivity filter sequence (gold) and inner helix glycine hinge (red) match colors used in the structures. Adapted from (Jiang *et al.*, 2002b).

the membrane as their C-terminus is displaced laterally away from the pore axis by conformational changes in the gating ring. A glycine amino acid facilitates the bending in MthK by introducing a hinge point in the middle of the inner helix. Like MthK, KcsA and many other K^+ channels contain a glycine at the very same location; its conservation suggests that the inner helices move in a somewhat similar manner in many different K^+ channels (figure 14).

Gating domains convert a stimulus into pore opening. Further studies are needed to understand how the free energy of Ca^{2+} binding is converted into pore opening in the MthK channel. And the mechanistic details of ligand gating will vary from one channel type to the next because nature is very modular with ion channels, just like with other proteins. Gene sequences show us that a multitude of different domains can be found attached to the inner helices of different K^+ channels, allowing ions such as Ca^{2+} or Na^+, small organic molecules, and even regulatory proteins to control the conformational state of the pore and so gate the ion channel (http://www.ncbi.nlm.nih.gov/BLAST/) (Atkinson *et al.*, 1991; Schumacher *et al.*, 2001; Yuan *et al.*, 2003; Kubo *et al.*, 1993).

A fundamentally different kind of gating domain allows certain K^+, Na^+, Ca^{2+} and nonselective cation channels to open in response to membrane volt-

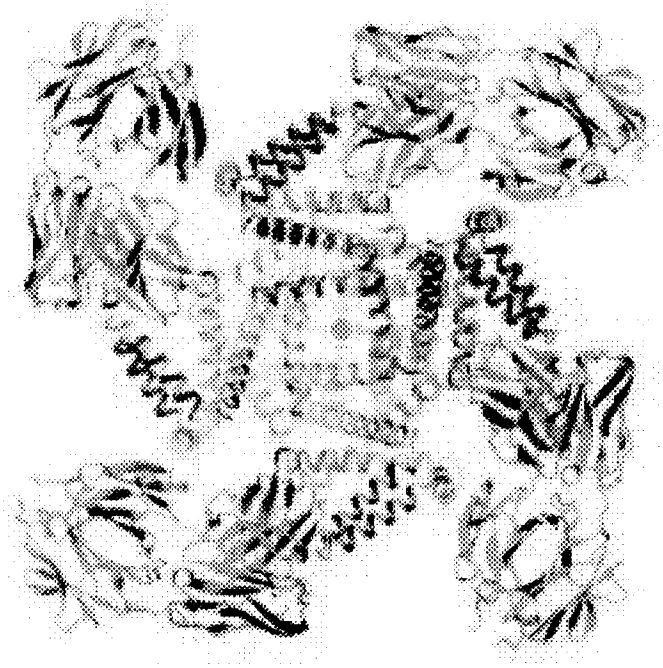

Figure 15. Crystal structure of the KvAP K^+ channel in complex with monoclonal antibody Fab fragments. The channel is viewed along the pore axis from the intracellular side of the membrane, with α-helical subunits colored in blue, yellow, cyan, and red. One Fab fragment (green) is bound to the helix-turn-helix element of the voltage sensor on each subunit. From (Jiang *et al.*, 2003a).

age changes. Referred to as voltage sensors, these domains are connected to the outer helices of the pore and form a structural unit within the membrane. The basic principle of operation for a voltage sensor is the movement of protein charges through the membrane electric field coupled to pore opening (Armstrong and Bezanilla, 1974; Sigworth, 1994; Bezanilla, 2000). Like transistors in an electronic device, voltage-dependent channels are electrical switches. They are a serious challenge for crystallographic analysis because of their conformational flexibility. Youxing Jiang and I working with Alice Lee and Jiayun Chen solved the structure of a voltage-dependent K^+ channel, KvAP, from the thermophilic Archea *Aeropyrum pernix* (Ruta *et al.*, 2003; Jiang *et al.*, 2003a) (figure 15). In the crystal of KvAP the voltage sensors, held by monoclonal Fab fragments, adopted a non-native conformation. This observation in itself is meaningful as it underscores the intrinsic flexibility of voltage sensors: in contrast Fab fragments had little effect on the more rigid KcsA K^+ channel and ClC Cl^- channel homolog, both of which we determined in the presence and absence of Fab fragments (Doyle *et al.*, 1998; Zhou *et al.*, 2001b; Dutzler *et al.*, 2002; Dutzler *et al.*, 2003). KvAP's voltage sensors contain a hydrophobic helix-turn-helix element with arginine residues beside the pore (Jiang *et al.*, 2003a), and functional experiments using tethered bi-

otin and avidin show that this element moves relative to the plane of the membrane (Jiang *et al.*, 2003b). Additional structures revealing different channel conformations will be needed to better understand the mechanistic details of voltage-dependent gating. But the KvAP structure and associated functional studies have provided a conceptual model for voltage-dependent gating – one in which the voltage sensors move at the protein-lipid interface in response to a balance between hydrophobic and electrostatic forces. Rees and colleagues at the California Institute of Technology determined the structure of a voltage regulated mechanosensitive channel called MscS, and although it is unrelated to traditional voltage-dependent channels, it too contains hydrophobic helix-turn-helix elements with arginine residues apparently against the lipid membrane (Bass *et al.*, 2002). MscS and KvAP are fascinating membrane protein structures. They do not fit into the standard category of membrane proteins with rigid hydrophobic walls against the lipid membrane core. I find such proteins intriguing.

We are only just beginning to understand the structural principles of ion channel gating and regulation. Electrophysiological studies have uncovered a multitude of connections between cellular biochemical pathways and ion channel function (Hille, 2001). New protein structures are now beginning to do the same. Beta subunits of certain eukaryotic voltage-dependent channels are structurally related to oxido-reductase enzymes (Gulbis *et al.*, 1999; Gulbis *et al.*, 2000). PAS domains on other K^+ channels belong to a family of sensory molecules (Morais Cabral *et al.*, 1998), and a specialized structure on G protein-gated channels forms a binding site for regulatory G protein subunits (Nishida and MacKinnon, 2002). The interconnectedness of ion channel function with many aspects of cell function is beginning to reveal itself as complex and fascinating.

CONCLUDING REMARKS

I think the most exciting time in ion channel studies is just beginning. So many of the important questions are waiting to be answered and we have the tools in hand to answer them. I am very optimistic about the future, and for the great possibilities awaiting young scientists who are now setting out to study ion channels and other membrane proteins. I consider myself very fortunate to have contributed to some small part of the knowledge we have today. Of course, my contributions would never have been possible without the efforts and enthusiasm of the young scientists who have come from around the world to study ion channels with me (figure 16). I also owe thanks to the Rockefeller University, the Howard Hughes Medical Institute, and the National Institutes of Health for supporting my scientific research.

MACKINNON LABORATORY: 1989–2003

Postdoctoral	*Students*	*Staff Scientists*	*Collaborators*
Laura Escobar	Lise Heginbotham	Tatiana Abramson	Gary Yellen
Zhe Lu	Michael Root	John Lewis	Maria Garcia
Adrian Gross	Patricia Hidalgo	Alice Lee MacKinnon	Gerhard Wagner
Kenton Swartz	Sanjay Aggarwal	Sabine Mann	Andrzej Krezel
Chul-Seung Park	James Morrell	Richard Pfuetzner	Brian Chait
Rama Ranganathan	Alexander Pico	Anling Kuo	Steve Cohen
Chinfei Chen	Vanessa Ruta	Minhui Long	Martine Cadene
Declan Doyle	Ian Berke	Amelia Kaufman	Benoit Roux
John Imredy		Ernest Campbell	Tom Muir
João Morais Cabral		Jiayun Chen	
Youxing Jiang			
Jacqueline Gulbis			
Raimund Dutzler			
Francis Valiyaveetil			
Xiao-Dan Pfenninger-Li			
Ming Zhou			
Ofer Yifrach			
Yufeng Zhou			
Sebastien Poget			
Motohiko Nishida			
Uta-Maria Ohndorf			
Steve Lockless			
Qiu-Xing Jiang			
Seok-Yong Lee			
Stephen Long			

Thanks to Rockefeller University, HHMI, NIH, to the synchrotrons CHESS, NSLS, ALS, APS and ESRF and to my assistant Wendell Chin.

Figure 16. MacKinnon laboratory from 1989 to 2003.

REFERENCE LIST

Accardi, A. and Miller, C. (2004) Proton-coupled chloride transport mediated by ClC-ec1, a bacterial homologue of the ClC chloride channels. Biophys.J. *86[1]*, 286a.

Armstrong, C. M. (1971). Interaction of tetraethylammonium ion derivatives with the potassium channels of giant axons. J. Gen. Physiol. *58*, 413–437.

Armstrong, C. M. (1981). Sodium channels and gating currents. Physiol. Rev. *61*, 645–683.

Armstrong, C. M. and Bezanilla,F. (1974). Charge movement associated with the opening and closing of the activation gates of the Na^+ channels. J. Gen. Physiol. *63*, 533–552.

Armstrong, C. M., Bezanilla, F., and Rojas, E. (1973). Destruction of sodium conductance inactivation in squid axons perfused with pronase. J. Gen. Physiol. *62*, 375–391.

Armstrong, C. M. and Hille, B. (1972). The inner quaternary ammonium ion receptor in potassium channels of the node of Ranvier. J. Gen. Physiol. *59*, 388–400.

Armstrong, C. M. (1974). Ionic pores, gates, and gating currents. Q. Rev. Biophys. *7*, 179–210.

Armstrong, C. M. and Bezanilla, F. (1977). Inactivation of the sodium channel. II. Gating current experiments. J. Gen. Physiol *70*, 567–590.

Atkinson, N. S., Robertson, G. A., and Ganetzky, B. (1991). A component of calcium-activated potassium channels encoded by the Drosophila slo locus. Science *253*, 551–555.

Bass, R. B., Strop, P., Barclay, M., and Rees, D. C. (2002). Crystal structure of *Escherichia coli* MscS, a voltage-modulated and mechanosensitive channel. Science *298*, 1582–1587.

Bezanilla, F. (2000). The voltage sensor in voltage-dependent ion channels. Physiol Rev. *80*, 555–592.

Cuello, L. G., Romero, J. G., Cortes, D .M., and Perozo, E. (1998). pH-dependent gating in the Streptomyces lividans K^+ channel. Biochemistry *37*, 3229–3236.

del Camino, D., Holmgren, M., Liu, Y., and Yellen, G. (2000). Blocker protection in the pore of a voltage-gated K^+ channel and its structural implications. Nature *403*, 321–325.

Dobler,v. M., Dunitz, J. D., and Kilbourn, B. T. (1969). Die struktur des KNCS-Komplexes von nonactin. Helvetica Chimica Acta *52*, 2573–2583.

Doyle, D. A., Morais Cabral, J. H., Pfuetzner, R. A., Kuo, A., Gulbis, J. M., Cohen, S. L., Chait, B. T., and MacKinnon,R. (1998). The structure of the potassium channel: molecular basis of K^+ conduction and selectivity. Science *280*, 69–77.

Dunitz, J. D. and Dobler, M. (1977). Structural studies of ionophores and their ion-complexes. In Biological aspects of inorganic chemistry, A. W. Addison, W. R. Cullen, D. Dolphin, and B. R. James, eds. John Wiley & Sons, Inc.), pp. 113–140.

Dutzler, R., Campbell, E. B., Cadene, M., Chait, B. T., and MacKinnon,R. (2002). X-ray structure of a ClC chloride channel at 3.0 Å reveals the molecular basis of anion selectivity. Nature *415*, 287–294.

Dutzler, R., Campbell, E. B., and MacKinnon, R. (2003). Gating the selectivity filter in ClC chloride channels. Science *300*, 108–112.

Garcia, M. L., Garcia-Calvo, M., Hidalgo, P., Lee, A., and MacKinnon, R. (1994). Purification and charaterization of three inhibitors of voltage-dependent K^+ channels from Leiurus quinquestriatus var. hebraeus venom. Biochemistry *33*, 6834–6839.

Gulbis, J. M., Mann, S., and MacKinnon, R. (1999). Structure of a voltage-dependent K^+ channel beta subunit. Cell *97*, 943–952.

Gulbis, J. M., Zhou, M., Mann, S., and MacKinnon, R. (2000). Structure of the cytoplasmic β subunit-T1 assembly of voltage-dependent K^+ channels. Science *289*, 123–127.

Heginbotham, L., Abramson, T., and MacKinnon, R. (1992). A functional connection between the pores of distantly related ion channels as revealed by mutant K^+ channels. Science *258*, 1152–1155.

Heginbotham, L., Lu, Z., Abramson, T., and MacKinnon, R. (1994). Mutations in the K^+ channel signature sequence. Biophys. J. *66*, 1061–1067.

Heginbotham, L., Kolmakova-Partensky, L., and Miller, C. (1998). Functional reconstitution of a prokaryotic K^+ channel. J. Gen. Physiol. *111*, 741–749.

Hidalgo, P. and MacKinnon, R. (1995). Revealing the architecture of a K^+ channel pore through mutant cycles with a peptide inhibitor. Science *268*, 307–310.

Hille, B. (1970). Ionic channels in nerve membranes. Prog. Biophys. Mol. Biol. *21*, 1–32.

Hille, B. (1973). Potassium channels in myelinated nerve. Selective permeability to small cations. J. Gen. Physiol. *61*, 669–686.

Hille, B. (2001). Ion Channels of Excitable Membranes. (Sunderland, MA: Sinauer Associates, Inc.).

Hille, B. (1971). The permeability of the sodium channel to organic cations in myelinated nerve. J. Gen. Physiol. *58*, 599–619.

Hodgkin, A. L. and Huxley, A. F. (1952a). A quantitative description of membrane current and its application to conduction and excitation in nerve. J. Physiol. *117*, 500–544.

Hodgkin, A. L. and Huxley, A. F. (1952b). Currents carried by sodium and potassium ions through the membrane of the giant axon of Loligo. J. Physiol. *116*, 449–472.

Hodgkin, A. L. and Huxley, A. F. (1952c). The components of membrane conductance in the giant axon of Loligo. J. Physiol. *116*, 473–496.

Hodgkin, A. L. and Huxley, A. F. (1952d). The dual effect of membrane potential on sodium conductance in the giant axon of Loligo. J. Physiol. *116*, 497–506.

Hodgkin, A. L. and Keynes, R. D. (1955). The potassium permeability of a giant nerve fibre. J. Physiol. (Lond) *128*, 61–88.

Jencks, W. P. (1987). Catalysis in Chemistry and Enzymology. (Dover Publications, Inc.).

Jentsch, T. J., Friedrich, T., Schriever, A., and Yamada, H. (1999). The CLC chloride channel family. Pflugers Arch. *437*, 783–795.

Jiang, Y., Lee, A., Chen, J., Ruta, V., Cadene, M., Chait, B., and MacKinnon, R. (2003a). X-ray structure of a voltage-dependent K^+ channel. Nature *423*, 33–41.

Jiang, Y., Ruta, V., Chen, J., Lee, A., and MacKinnon, R. (2003b). The principle of gating charge movement in a voltage-dependent K^+ channel. Nature *423*, 42–48.

Jiang, Y., Lee, A., Chen, J., Cadene, M., Chait, B. T., and MacKinnon, R. (2002a). Crystal structure and mechanism of a calcium-gated potassium channel. Nature *417*, 515–522.

Jiang, Y., Lee, A., Chen, J., Cadene, M., Chait, B. T., and MacKinnon, R. (2002b). The open pore conformation of potassium channels. Nature *417*, 523–526.

Jiang, Y., Pico, A., Cadene, M., Chait, B. T., and MacKinnon, R. (2001). Structure of the RCK domain from the *E. coli* K^+ channel and demonstration of its presence in the human BK channel. Neuron *29*, 593–601.

Kamb, A., Iverson, L. E., and Tanouye, M. A. (1987). Molecular characterization of Shaker, a Drosophila gene that encodes a potassium channel. Cell *50*, 405–413.

Kubo, Y., Reuveny, E., Slesinger, P. A., Jan, Y. N., and Jan, L. Y. (1993). Primary structure and functional expression of a rat G-protein-coupled muscarinic potassium channel. Nature *364*, 802–806.

MacKinnon, R. (1991). Determination of the subunit stoichiometry of a voltage-activated potassium channel. Nature *350*, 232–235.

MacKinnon, R. (1995). Pore loops: an emerging theme in ion channel structure. Neuron *14*, 889–892.

MacKinnon, R., Cohen, S. L., Kuo, A., Lee, A., and Chait, B. T. (1998). Structural conservation in prokaryotic and eukaryotic potassium channels. Science *280*, 106–109.

MacKinnon, R. and Miller, C. (1988). Mechanism of charybdotoxin block of the high-conductance, Ca^{2+}-activated K^+ channel. J. Gen. Physiol. *91*, 335–349.

MacKinnon, R. and Miller, C. (1989). Mutant potassium channels with altered binding of charybdotoxin, a pore-blocking peptide inhibitor. Science *245*, 1382–1385.

MacKinnon, R., Reinhart, P. H., and White, M. M. (1988). Charybdotoxin block of Shaker K^+ channels suggests that different types of K^+ channels share common structural features. Neuron *1*, 997–1001.

MacKinnon, R. and Yellen G. (1990). Mutations affecting TEA blockade and ion permeation in voltage-activated K^+ channels. Science *250*, 276–279.

Maduke, M., Miller, C., and Mindell, J. A. (2000). A decade of CLC chloride channels: structure, mechanism, and many unsettled questions. Annu. Rev. Biophys. Biomol. Struct. *29*, 411–438.

Milkman, R. (1994). An *Escherichia coli* homologue of eukaryotic potassium channel proteins. Proc. Natl. Acad. Sci. 91[9], 3510–3514.

Morais-Cabral, J. H., Zhou, Y., and MacKinnon, R. (2001). Energetic optimization of ion conduction rate by the K^+ selectivity filter. Nature *414*, 37–42.

Morais-Cabral, J. H., Lee, A., Cohen, S. L., Chait, B. T., Li, M., and MacKinnon, R. (1998). Crystal structure and functional analysis of the HERG potassium channel N-terminus: a eukaryotic PAS domain. Cell *95*, 649–655.

Neher, E. and Sakmann, B. (1976). Single-channel currents recorded from membrane of denervated frog muscle fibres. Nature *260*, 799–802.

Nishida, M. and MacKinnon, R. (2002). Structural basis of inward rectification: Cytoplasmic pore of the G protein-gated inward rectifier GIRKI at 1.8 Å resolution. Cell *III*, 957–965.

Perozo, E., Cortes, D. M., and Cuello, L. G. (1999). Structural rearrangements underlying K^+-channel activation gating. Science *285*, 73–78.

Pongs, O., Kecskemethy, N., Muller, R., Krah-Jentgens, I., Baumann, A., Kiltz, H. H., Canal, I., Llamazares, S., and Ferrus, A. (1988). Shaker encodes a family of putative potassium channel proteins in the nervous system of *Drosophila*. EMBO J. *7*, 1087–1096.

Ranganathan, R., Lewis, J. H., and MacKinnon, R. (1996). Spatial localization of the K^+ channel selectivity filter by mutant cycle-based structure analysis. Neuron *16*, 131–139.

Roux, B. and MacKinnon, R. (1999). The cavity and pore helices in the KcsA K^+ channel: electrostatic stabilization of monovalent cations. Science *285*, 100–102.

Ruta, V., Jiang, Y., Lee, A., Chen, J., and MacKinnon, R. (2003). Functional analysis of an archeabacterial voltage-dependent K^+ channel. Nature *422*, 180–185.

Schrempf, H., Schmidt, O., Kummerlen, R., Hinnah, S., Muller, D., Betzler, M., Steinkamp, T., and Wagner, R. (1995). A prokaryotic potassium ion channel with two predicted transmembrane segments from *Streptomyces lividans*. EMBO J. *14*, 5170–5178.

Schumacher, M. A., Rivard, A. F., Bachinger, H. P., and Adelman, J. P. (2001). Structure of the gating domain of a Ca2+-activated K^+ channel complex with Ca^{2+}/calmodulin. Nature *410*, 1120–1124.

Sigworth, F. J. (1994). Voltage gating of ion channels. Q. Rev. Biophys. *27*, 1–40.

Tempel, B. L., Papazian, D. M., Schwarz, T. L., Jan, Y. N., and Jan, L. Y. (1987). Sequence of a probable potassium channel component encoded at Shaker locus of *Drosophila*. Science *237*, 770–775.

Yellen, G. Jurman, M. E., Abramson, T., and MacKinnon, R. (1991). Mutations affecting internal TEA blockade identify the probable pore-forming region of a K^+ channel. Science *251*, 939–942.

Yuan, A., Santi, C. M., Wei, A., Wang, Z. W., Pollak, K., Nonet, M., Kaczmarek, L., Crowder, C. M., and Salkoff, L. (2003). The sodium-activated potassium channel is encoded by a member of the Slo gene family. Neuron *37*, 765–773.

Zhou, M. and MacKinnon, R. (2004). A mutant KcsA K^+ channel with altered conduction properties and selectivity filter ion distribution. J.Mol.Biol. 338, 839–846.

Zhou, M., Morais-Cabral, J. H., Mann, S., and MacKinnon, R. (2001a). Potassium channel receptor site for the inactivation gate and quaternary amine inhibitors. Nature *411*, 657–661.

Zhou, Y. and MacKinnon, R. (2003). The occupancy of ions in the K^+ selectivity filter: Charge balance and coupling of ion binding to a protein conformational change underlie high conduction rates. J. Mol. Biol. *333*, 965–975.

Zhou, Y., Morais-Cabral, J. H., Kaufman, A., and MacKinnon, R. (2001b). Chemistry of ion coordination and hydration revealed by a K^+ channel- Fab complex at 2.0 Å resolution. Nature *414*, 43–48.

EXHIBIT 6

Guidance for Industry

Dissolution Testing of Immediate Release Solid Oral Dosage Forms

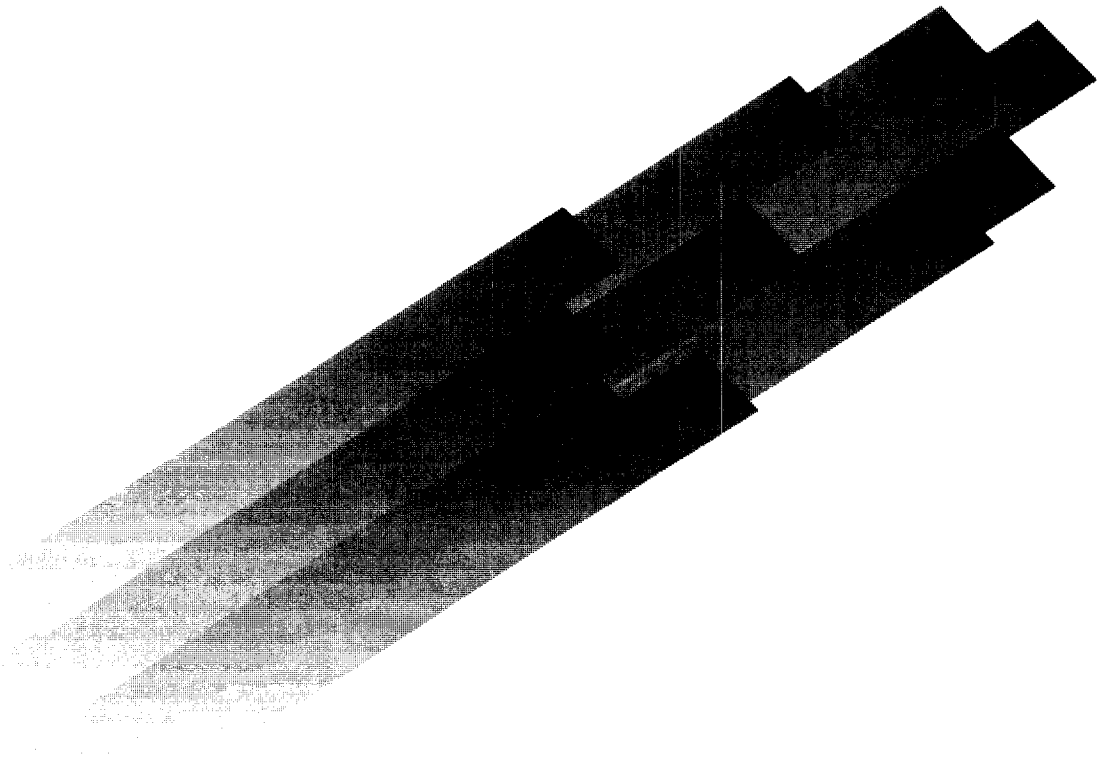

U.S. Department of Health and Human Services
Food and Drug Administration
Center for Drug Evaluation and Research (CDER)
August 1997

BP 1

Guidance for Industry

Dissolution Testing of Immediate Release Solid Oral Dosage Forms

Additional copies are available from:

Office of Training and Communications
Division of Communications Management
The Drug Information Branch, HFD-210
5600 Fishers Lane
Rockville, MD 20857

(Tel) 301-827-4573
(Internet) http://www.fda.gov/cder/guidance.htm

U.S. Department of Health and Human Services
Food and Drug Administration
Center for Drug Evaluation and Research (CDER)
August 1997

BP 1

Table of Contents

GUIDANCE FOR INDUSTRY[1]

Dissolution Testing of Immediate Release Solid Oral Dosage Forms

I. INTRODUCTION

This guidance is developed for immediate release (IR) dosage forms and is intended to provide (1) general recommendations for dissolution testing; (2) approaches for setting dissolution specifications related to the biopharmaceutic characteristics of the drug substance; (3) statistical methods for comparing dissolution profiles; and (4) a process to help determine when dissolution testing is sufficient to grant a waiver for an in vivo bioequivalence study. This document also provides recommendations for dissolution tests to help ensure continuous drug product quality and performance after certain postapproval manufacturing changes. Summary information on dissolution methodology, apparatus, and operating conditions for dissolution testing of IR products is provided in summary form in Appendix A. This guidance is intended to complement the SUPAC - IR guidance for industry: *Immediate Release Solid Oral Dosage Forms: Scale-up and Post-Approval Changes: Chemistry, Manufacturing and Controls, In Vitro Dissolution Testing, and In Vivo Bioequivalence Documentation*, with specific reference to the generation of dissolution profiles for comparative purposes.

II. BACKGROUND

Drug absorption from a solid dosage form after oral administration depends on the release of the drug substance from the drug product, the dissolution or solubilization of the drug under physiological conditions, and the permeability across the gastrointestinal tract. Because of the critical nature of the first two of these steps, in vitro dissolution may be relevant to the prediction of in vivo performance. Based on this general consideration, in vitro dissolution tests for immediate release solid oral dosage forms, such as tablets and capsules, are used to (1) assess the lot-to-lot quality of a drug product; (2) guide development of new formulations;

---

[1]This guidance has been prepared by the Immediate Release Expert Working Group of the Biopharmaceutics Coordinating Committee in the Center for Drug Evaluation and Research (CDER) at the Food and Drug Administration. This guidance document represents the Agency's current thinking on the dissolution testing of immediate release solid oral dosage forms. It does not create or confer any rights for or on any person and does not operate to bind FDA or the public. An alternative approach may be used if such approach satisfies the requirements of the applicable statute, regulations, or both.

and (3) ensure continuing product quality and performance after certain changes, such as changes in the formulation, the manufacturing process, the site of manufacture, and the scale-up of the manufacturing process.

Current knowledge about the solubility, permeability, dissolution, and pharmacokinetics of a drug product should be considered in defining dissolution test specifications for the drug approval process. This knowledge should also be used to ensure continued equivalence of the product, as well as to ensure the product's *sameness* under certain scale-up and postapproval changes.

New drug applications (NDAs) submitted to the Food and Drug Administration (FDA) contain bioavailability data and in vitro dissolution data, that, together with chemistry, manufacturing, and controls (CMC) data, characterize the quality and performance of the drug product. In vitro dissolution data are generally obtained from batches that have been used in pivotal clinical and/or bioavailability studies and from other human studies conducted during product development. Acceptable bioequivalence data and comparable in vitro dissolution and CMC data are required for approval of abbreviated new drug applications (ANDAs) (21 CFR 314.94). The in vitro specifications for generic products should be established based on a dissolution profile. For new drug applications, as well as generic drug applications, the dissolution specifications should be based on acceptable clinical, bioavailability, and/or bioequivalence batches.

Once the specifications are established in an NDA, the dissolution specifications for batch-to-batch quality assurance are published in the *United States Pharmacopeia* (USP) as compendial standards, which become the official specifications for all subsequent IR products with the same active ingredients. In general, these compendial dissolution standards are single-point dissolution tests, not profiles.

III. BIOPHARMACEUTICS CLASSIFICATION SYSTEM

Based on drug solubility and permeability, the following Biopharmaceutics Classification System (BCS) is recommended in the literature (Amidon 1995):

Case 1:	High Solubility - High Permeability Drugs
Case 2:	Low Solubility - High Permeability Drugs
Case 3:	High Solubility - Low Permeability Drugs
Case 4:	Low Solubility - Low Permeability Drugs

This classification can be used as a basis for setting in vitro dissolution specifications and can also provide a basis for predicting the likelihood of achieving a successful in vivo-in vitro correlation (IVIVC). The solubility of a drug is determined by dissolving the highest unit dose of the drug in 250 mL of buffer adjusted between pH 1.0 and 8.0. A drug substance is considered highly soluble when the dose/solubility volume of solution are less than or equal to 250 mL. High-permeability drugs are generally those with an extent of absorption that is greater than 90% in the absence of

documented instability in the gastrointestinal tract or those whose permeability has been determined experimentally. The BCS suggests that for high solubility, high permeability (case 1) drugs and in some instances for high solubility, low permeability (case 3) drugs, 85% dissolution in 0.1N HCl in 15 minutes can ensure that the bioavailability of the drug is not limited by dissolution. In these cases, the rate limiting step for drug absorption is gastric emptying.

The mean T50% gastric residence (emptying) time is 15-20 minutes under fasting conditions. Based on this information, a conservative conclusion is that a drug product undergoing 85% dissolution in 15 minutes under mild dissolution test conditions in 0.1N HCl behaves like a solution and generally should not have any bioavailability problems. If the dissolution is slower than gastric emptying, a dissolution profile with multiple time points in multimedia is recommended.

In the case of low solubility/high permeability drugs (case 2), drug dissolution may be the rate limiting step for drug absorption and an IVIVC may be expected. A dissolution profile in multiple media is recommended for drug products in this category. In the case of high solubility/low permeability drugs (case 3), permeability is the rate controlling step and a limited IVIVC may be possible, depending on the relative rates of dissolution and intestinal transit. Drugs in case 4 (i.e., low solubility/low permeability drugs) present significant problems for oral drug delivery.

IV. SETTING DISSOLUTION SPECIFICATIONS

In vitro dissolution specifications are established to ensure batch-to-batch consistency and to signal potential problems with in vivo bioavailability. For NDAs, the dissolution specifications should be based on acceptable clinical, pivotal bioavailability, and/or bioequivalence batches. For ANDAs/AADAs, the dissolution specifications should be based on the performance of acceptable bioequivalence batches of the drug product. The NDA dissolution specifications should be based on experience gained during the drug development process and the in vitro performance of appropriate test batches. In the case of a generic drug product, the dissolution specifications are generally the same as the reference listed drug (RLD). The specifications are confirmed by testing the dissolution performance of the generic drug product from an acceptable bioequivalence study. If the dissolution of the generic product is substantially different compared to that of the reference listed drug and the in vivo data remain acceptable, a different dissolution specification for the generic product may be set. Once a dissolution specification is set, the drug product should comply with that specification throughout its shelf life.

The International Conference on Harmonisation (ICH) Q1A guideline (*Stability Testing of New Drug Substances and Drug Products*) has recommended that for an NDA, three batches (two pilot and one smaller scale) be placed into stability testing. These batches also may be used to set dissolution specifications when a suitable bioequivalence relationship exists between these batches and both the pivotal clinical trial batch and the drug product intended for the market.

Three catagories of dissolution test specifications for immediate release drug products are described in the guidance.

- Single-point specifications

  As a routine quality control test. (For highly soluble and rapidly dissolving drug products.)

- Two-point specifications

  1. For characterizing the quality of the drug product.

  2. As a routine quality control test for certain types of drug products (e.g., slow dissolving or poorly water soluble drug product like carbamazepine).

- Dissolution profile comparison

  1. For accepting product sameness under SUPAC-related changes.

  2. To waive bioequivalence requirements for lower strengths of a dosage form.

  3. To support waivers for other bioequivalence requirements.

In the future, a two-time point approach may be useful, both to characterize a drug product and to serve as quality control specification.

A. Approaches for Setting Dissolution Specifications for a New Chemical Entity

Dissolution methodology and specifications developed by a sponsor are presented in the biopharmaceutics section (21 CFR 320.24(b)(5)), and the chemistry, manufacturing, and controls section (21 CFR 314.50(d)(1)(ii)(a)) of an NDA. The dissolution characteristics of the drug product should be developed based on consideration of the pH solubility profile and pKa of the drug substance. The drug permeability or octanol/water partition coefficient measurement may be useful in selecting the dissolution methodology and specifications. The dissolution specifications are established in consultation with biopharmaceutics and CMC review staff in the Office of Pharmaceutical Science (OPS). For NDAs, the specifications should be based on the dissolution characteristics of batches used in pivotal clinical trials and/or in confirmatory bioavailability studies. If the formulation intended for marketing differs significantly from the drug product used in pivotal clinical trials, dissolution and bioequivalence testing between the two formulations are recommended.

Dissolution testing should be carried out under mild test conditions, basket method at 50/100 rpm or paddle method at 50/75 rpm, at 15-minute intervals, to generate a dissolution profile. For rapidly dissolving products, generation of an adequate profile sampling at 5- or 10-minute intervals may be necessary. For highly soluble and rapidly dissolving drug products (BCS classes 1 and 3), a single-point dissolution test specification of NLT 85% (Q=80%) in 60 minutes or less is sufficient as a routine quality control test for batch-to-batch uniformity. For slowly dissolving or poorly water soluble drugs (BCS class 2), a two-point dissolution specification, one at 15 minutes to include a dissolution range (a dissolution window) and the other at a later point (30, 45, or 60 minutes) to ensure 85% dissolution, is recommended to characterize the quality of the product. The product is expected to comply with dissolution specifications throughout its shelf life. If the dissolution characteristics of the drug product change with time, whether or not the specifications should be altered will depend on demonstrating bioequivalence of the changed product to the original biobatch or pivotal batch. To ensure continuous batch-to-batch equivalence of the product after scale-up and postapproval changes in the marketplace, dissolution profiles should remain comparable to those of the approved biobatch or pivotal clinical trial batch(es).

B. Approaches for Setting Dissolution Specifications for Generic Products

The approaches for setting dissolution specifications for generic products fall into three categories, depending on whether an official compendial test for the drug product exists and on the nature of the dissolution test employed for the reference listed drug. All approved new drug products should meet current USP dissolution test requirements, if they exist. The three categories are:

1. USP Drug Product Dissolution Test Available

In this instance, the quality control dissolution test is the test described in the USP. The Division of Bioequivalence, Office of Generic Drugs, also recommends taking a dissolution profile at 15-minute intervals or less using the USP method for test and reference products (12 units each). The Division of Bioequivalence may also recommend submitting additional dissolution data when scientifically justified. Examples of this include (1) cases in which USP does not specify a dissolution test for all active drug substances of a combination product and (2) cases in which USP specifies use of disintegration apparatus.

2. USP Drug Product Dissolution Test Not Available; Dissolution Test for Reference Listed NDA Drug Product Publicly Available

In this instance, a dissolution profile at 15-minute intervals of test and reference products (12 units each) using the method approved for the reference listed product is recommended. The Division of Bioequivalence may also request

submission of additional dissolution testing data as a condition of approval, when scientifically justified.

3. USP Drug Product Dissolution Test Not Available; Dissolution Test for Reference Listed NDA Drug Product Not Publicly Available

In this instance, comparative dissolution testing using test and reference products under a variety of test conditions is recommended. The test conditions may include different dissolution media (pH 1 to 6.8), addition of surfactant, and use of apparatus 1 and 2 with varying agitation. In all cases, profiles should be generated as previously recommended. The dissolution specifications are set based on the available bioequivalence and other data.

C. Special Cases

1. Two-Point Dissolution Test

For poorly water soluble drug products (e.g., carbamazapine), dissolution testing at more than one time point for routine quality control is recommended to ensure in vivo product performance. Alternatively, a dissolution profile may be used for purposes of quality control.

2. Two-Tiered Dissolution Test

To more accurately reflect the physiologic conditions of the gastrointestinal tract, two-tiered dissolution testing in simulated gastric fluid (SGF) with and without pepsin or simulated intestinal fluid (SIF) with and without pancreatin may be employed to assess batch-to-batch product quality provided the bioequivalence is maintained.

Recent examples involving soft and hard gelatin capsules show a decrease in the dissolution profile over time either in SGF or in SIF without enzymes. This has been attributed to pellicle formation. When the dissolution of aged or slower releasing capsules was carried out in the presence of an enzyme (pepsin in SGF or pancreatin in SIF), a significant increase in the dissolution was observed. In this setting, multiple dissolution media may be necessary to adequately assess product quality.

D. Mapping or Response Surface Methodology

Mapping is defined as a process for determining the relationship between critical manufacturing variables (CMV) and a response surface derived from an in vitro dissolution profile and an in vivo bioavailability data set. The CMV include changes in the

formulation, process, equipment, materials, and methods for the drug product that can significantly affect in vitro dissolution (Skelly 1990, Shah 1992). The goal is to develop product specifications that will ensure bioequivalence of future batches prepared within the limits of acceptable dissolution specifications. Several experimental designs are available to study the influence of CMV on product performance. One approach to study and evaluate the mapping process includes (1) prepare two or more dosage formulations using CMV to study their in vitro dissolution characteristics; (2) test the products with fastest and slowest dissolution characteristics along with the standard or the *to be marketed dosage form* in small groups (e.g., $n \geq 12$) of human subjects; and (3) determine the bioavailability of the products and in vitro-in vivo relationship. The products with extreme dissolution characteristics are also referred to as *side batches* (Siewert 1995). If the products with the extreme range of dissolution characteristics are found to be bioequivalent to the standard or the *to be marketed dosage form*, future batches with dissolution characteristics between these ranges should be equivalent to one another. This approach can be viewed as verifying the limits of the dissolution specifications. Product dissolution specifications established using a mapping approach will provide maximum likelihood of ensuring stable quality and product performance. Depending on the number of products evaluated, the mapping study can provide information on in vitro-in vivo correlations and/or a rank order relationship between in vivo and in vitro data.

E. In Vivo-In Vitro Correlations

For highly water soluble (BCS classes 1 and 3) immediate release products using currently available excipients and manufacturing technology, an IVIVC may not be possible. For poorly water soluble products, BCS class 2, an IVIVC may be possible.

The value of dissolution as a quality control tool for predicting in vivo performance of a drug product is significantly enhanced if an in vitro-in vivo relationship (correlation or association) is established. The in vitro test serves as a tool to distinguish between acceptable and unacceptable drug products. Acceptable products are bioequivalent, in terms of in vivo performance, whereas unacceptable products are not. To achieve an in vitro-in vivo correlation, at least three batches that differ in the in vivo as well as the in vitro performance should be available. If the batches show differences in in vivo performance, then in vitro test conditions can be modified to correspond with the in vivo data to achieve an in vitro-in vivo correlation. If no difference is found in the in vivo performance of the batches and if the in vitro performance is different, it may be possible to modify test conditions to achieve the same dissolution performance of the batches studied in vivo. Very often, the in vitro dissolution test is found to be more sensitive and discriminating than the in vivo test. From a quality assurance point of view, a more discriminative dissolution method is preferred, because the test will indicate possible changes in the quality of the product before in vivo performance is affected.

F. Validation and Verification of Specifications

Confirmation by in vivo studies may be needed for validation of an in vitro system. In this situation, the same formulation should be used but nonformulation CMV should be varied. Two batches with different in vitro profiles should be prepared (mapping approach). These products should then be tested in vivo. If the two products show different in vivo characteristics, then the system is validated. In contrast, if there is no difference in the in vivo performance, the results can be interpreted as verifying the dissolution specification limits as discussed under mapping. Thus, either validation or verification of dissolution specifications should be confirmed.

V. DISSOLUTION PROFILE COMPARISONS

Until recently, single-point dissolution tests and specifications have been employed in evaluating scale-up and postapproval changes, such as (1) scale-up, (2) manufacturing site changes, (3) component and composition changes, and (4) equipment and process changes. A *changed product* may also be a lower strength of a previously approved drug product. In the presence of certain minor changes, the single-point dissolution test may be adequate to ensure unchanged product quality and performance. For more major changes, a dissolution profile comparison performed under identical conditions for the product before and after the change(s) is recommended (see SUPAC-IR). Dissolution profiles may be considered similar by virtue of (1) overall profile similarity and (2) similarity at every dissolution sample time point. The dissolution profile comparison may be carried out using model independent or model dependent methods.

A. Model Independent Approach Using a Similarity Factor

A simple model independent approach uses a difference factor (f_1) and a similarity factor (f_2) to compare dissolution profiles (Moore 1996). The difference factor (f_1) calculates the percent (%) difference between the two curves at each time point and is a measurement of the relative error between the two curves:

$$f_1 = \{[\sum_{t=1}^{n} | R_t - T_t |]/[\sum_{t=1}^{n} R_t]\} \bullet 100$$

where n is the number of time points, R_t is the dissolution value of the reference (prechange) batch at time t, and T_t is the dissolution value of the test (postchange) batch at time t.

The similarity factor (f_2) is a logarithmic reciprocal square root transformation of the sum of squared error and is a measurement of the similarity in the percent (%) dissolution between the two curves.

$$f_2 = 50 \bullet \log \{[1+(1/n)\sum_{t=1}^{n} (R_t - T_t)^2]^{-0.5} \bullet 100\}$$

A specific procedure to determine difference and similarity factors is as follows:

1. Determine the dissolution profile of two products (12 units each) of the test (postchange) and reference (prechange) products.

2. Using the mean dissolution values from both curves at each time interval, calculate the difference factor (f_1) and similarity factor (f_2) using the above equations.

3. For curves to be considered similar, f_1 values should be close to 0, and f_2 values should be close to 100. Generally, f_1 values up to 15 (0-15) and f_2 values greater than 50 (50-100) ensure sameness or equivalence of the two curves and, thus, of the performance of the test (postchange) and reference (prechange) products.

This model independent method is most suitable for dissolution profile comparison when three to four or more dissolution time points are available. As further suggestions for the general approach, the following recommendations should also be considered:

- The dissolution measurements of the test and reference batches should be made under exactly the same conditions. The dissolution time points for both the profiles should be the same (e.g., 15, 30, 45, 60 minutes). The reference batch used should be the most recently manufactured prechange product.

- Only one measurement should be considered after 85% dissolution of both the products.

- To allow use of mean data, the percent coefficient of variation at the earlier time points (e.g., 15 minutes) should not be more than 20%, and at other time points should not be more than 10%.

- The mean dissolution values for R_t can be derived either from (1) last prechange (reference) batch or (2) last two or more consecutively manufactured prechange batches.

B. Model Independent Multivariate Confidence Region Procedure

In instances where within batch variation is more than 15% CV, a multivariate model independent procedure is more suitable for dissolution profile comparison. The following steps are suggested:

1. Determine the similarity limits in terms of multivariate statistical distance (MSD) based on interbatch differences in dissolution from reference (standard approved) batches.

2. Estimate the MSD between the test and reference mean dissolutions.

3. Estimate 90% confidence interval of true MSD between test and reference batches.

4. Compare the upper limit of the confidence interval with the similarity limit. The test batch is considered similar to the reference batch if the upper limit of the confidence interval is less than or equal to the similarity limit.

C. Model Dependent Approaches

Several mathematical models have been described in the literature to fit dissolution profiles. To allow application of these models to comparison of dissolution profiles, the following procedures are suggested:

1. Select the most appropriate model for the dissolution profiles from the standard, prechange, approved batches. A model with no more than three parameters (such as linear, quadratic, logistic, probit, and Weibull models) is recommended.

2. Using data for the profile generated for each unit, fit the data to the most appropriate model.

3. A similarity region is set based on variation of parameters of the fitted model for test units (e.g., capsules or tablets) from the standard approved batches.

4. Calculate the MSD in model parameters between test and reference batches.

5. Estimate the 90% confidence region of the true difference between the two batches.

6. Compare the limits of the confidence region with the similarity region. If the confidence region is within the limits of the similarity region, the test batch is considered to have a similar dissolution profile to the reference batch.

VI. DISSOLUTION AND SUPAC-IR

The SUPAC-IR guidance defines the levels of changes, recommended tests, and filing documentation to ensure product quality and performance of reference (prechange product) with postapproval changes in (1) components and composition, (2) site of manufacturing, (3) the scale of manufacturing, and (4) process and equipment changes in the manufacturing of immediate release products (FDA 1995). Depending on the level of change and the biopharmaceutics classification system of the active drug substance, the SUPAC-IR guidance recommends different levels of in vitro dissolution test and/or in vivo bioequivalence studies. Tests vary depending on therapeutic range and solubility and permeability factors of the drug substance. For formulation changes beyond those listed in the guidance, additional dissolution profile determinations in several media are recommended. For manufacturing site changes, scale-up equipment changes, and minor process changes, only dissolution testing should be sufficient to ensure unchanged product quality and performance. The SUPAC-IR guidance recommends dissolution profile comparisons for approving different levels of changes and documenting product *sameness* between the test (postchange) and reference (prechange) product. It recommends dissolution profile comparisons using a model independent approach and the similarity factor (f_2).

VII. BIOWAIVERS

In addition to routine quality control tests, comparative dissolution tests have been used to waive bioequivalence requirements (biowaivers) for lower strengths of a dosage form. For biowaivers, a dissolution profile should be generated and evaluated using one of the methods described under Section V in this guidance, "Dissolution Profile Comparisons." Biowaivers are generally provided for multiple strengths after approval of a bioequivalence study performed on one strength, using the following criteria:

For multiple strengths of IR products with linear kinetics, the bioequivalence study may be performed at the highest strength and waivers of in vivo studies may be granted on lower strengths, based on an adequate dissolution test, provided the lower strengths are proportionately similar in composition (21 CFR 320.22(d)(2)). *Similar* may also be interpreted to mean that the different strengths of the products are within the scope of changes permitted under the category "Components and Composition," discussed in the SUPAC-IR guidance. In all cases, the approval of additional strengths is based on dissolution profile comparisons between these additional strengths and the strength of the batch used in the pivotal bioequivalence study.

Appendix A
Dissolution Testing Conditions

Apparatus

The most commonly employed dissolution test methods are (1) the basket method (Apparatus 1) and (2) the paddle method (Apparatus 2) (Shah 1989). The basket and the paddle methods are simple, robust, well standardized, and used worldwide. These methods are flexible enough to allow dissolution testing for a variety of drug products. For this reason, the official in vitro dissolution methods described in *U.S. Pharmacopeia* (USP), Apparatus 1 and Apparatus 2 should be used unless shown to be unsatisfactory. The in vitro dissolution procedures, such as the reciprocating cylinder (Apparatus 3) and a flow-through cell system (Apparatus 4) described in the USP, may be considered if needed. These methodologies or other alternatives/modifications should be considered on the basis of their proven superiority for a particular product. Because of the diversity of biological and formulation variables and the evolving nature of understanding in this area, different experimental modifications may need to be carried out to obtain a suitable in vivo correlation with in vitro release data. Dissolution methodologies and apparatus described in the USP can generally be used either with manual sampling or with automated procedures.

Dissolution Medium

Dissolution testing should be carried out under physiological conditions, if possible. This allows interpretation of dissolution data with regard to in vivo performance of the product. However, strict adherence to the gastrointestinal environment need not be used in routine dissolution testing. The testing conditions should be based on physicochemical characteristics of the drug substance and the environmental conditions the dosage form might be exposed to after oral administration.

The volume of the dissolution medium is generally 500, 900, or 1000 mL. Sink conditions are desirable but not mandatory. An aqueous medium with pH range 1.2 to 6.8 (ionic strength of buffers the same as in USP) should be used. To simulate intestinal fluid (SIF), a dissolution medium of pH 6.8 should be employed. A higher pH should be justified on a case-by-case basis and, in general, should not exceed pH 8.0. To simulate gastric fluid (SGF), a dissolution medium of pH 1.2 should be employed without enzymes. The need for enzymes in SGF and SIF should be evaluated on a case-by-case basis and should be justified. Recent experience with gelatin capsule products indicates the possible need for enzymes (pepsin with SGF and pancreatin with SIF) to dissolve pellicles, if formed, to permit the dissolution of the drug. Use of water as a dissolution medium also is discouraged because test conditions such as pH and surface tension can vary depending on the source of water and may change during the dissolution test itself, due to the influence of the active and inactive ingredients. For water insoluble or sparingly water soluble drug products, use of a surfactant such as sodium lauryl sulfate is recommended (Shah 1989, 1995). The need for and the amount of the surfactant should be justified. Use of a hydro alcoholic medium is discouraged.

All dissolution tests for IR dosage forms should be conducted at 37±0.5°C. The basket and paddle method can be used for performing dissolution tests under multimedia conditions (e.g., the initial dissolution test can be carried out at pH 1.2, and, after a suitable time interval, a small amount of buffer can be added to raise pH to 6.8). Alternatively, if addition of an enzyme is desired, it can be added after initial studies (without enzymes). Use of Apparatus 3 allows easy change of the medium. Apparatus 4 can also be adopted for a change in dissolution medium during the dissolution run.

Certain drug products and formulations are sensitive to dissolved air in the dissolution medium and will need deaeration. In general, capsule dosage forms tend to float during dissolution testing with the paddle method. In such cases, it is recommended that a few turns of a wire helix (USP) around the capsule be used.

The apparatus suitability tests should be carried out with a performance standard (i.e., calibrators) at least twice a year and after any significant equipment change or movement. However, a change from basket to paddle or vice versa may need recalibration. The equipment and dissolution methodology should include the product related operating instructions such as deaeration of the dissolution medium and use of a wire helix for capsules. Validation of automated procedures compared to the manual procedures should be well documented. Validation of determinative steps in the dissolution testing process should comply with the set standards for analytical methodology.

Agitation

In general, mild agitation conditions should be maintained during dissolution testing to allow maximum discriminating power and to detect products with poor in vivo performance. Using the basket method, the common agitation (or stirring speed) is 50-100 rpm; with the paddle method, it is 50-75 rpm (Shah et al., 1992). Apparatus 3 and 4 are seldom used to assess the dissolution of immediate release drug products.

Validation

Validation of the dissolution apparatus/methodology should include (1) the system suitability test using calibrators; (2) deaeration, if necessary; (3) validation between manual and automated procedures; and (4) validation of a determinative step (i.e., analytical methods employed in quantitative analysis of dissolution samples). This should include all appropriate steps and procedures of analytical methods validation.

REFERENCES

Amidon, G. L., H. Lennernas, V. P. Shah, and J. R. Crison, 1995, "A Theoretical Basis For a Biopharmaceutic Drug Classification: The Correlation of In Vitro Drug Product Dissolution and In Vivo Bioavailability," *Pharmaceutical Research,* 12:413-420.

FDA, 1995, Center for Drug Evaluation and Research, *Guidance for Industry: Immediate Release Solid Oral Dosage Forms. Scale-up and Post-Approval Changes: Chemistry, Manufacturing and Controls, In Vitro Dissolution Testing, and In Vivo Bioequivalence Documentation* [SUPAC-IR], November 1995.

Meyer, M. C., A. B. Straughn, E. J. Jarvi, G. C. Wood, F. R. Pelsor, and V. P. Shah, 1992, "The Bioequivalence of Carbamazepine Tablets with a History of Clinical Failures," *Pharmaceutical Research,* 9:1612-1616.

Moore, J. W. and H. H. Flanner, 1996, "Mathematical Comparison of Dissolution Profiles," *Pharmaceutical Technology*, 20 (6):64-74.

Shah, V. P., et al., 1989, "In Vitro Dissolution Profile of Water Insoluble Drug Dosage Forms in the Presence of Surfactants," *Pharmaceutical Research,* 6:612-618.

Shah, V. P., et al., 1992, "Influence of Higher Rate of Agitation on Release Patterns of Immediate Release Drug Products," *Journal of Pharmaceutical Science,* 81:500-503.

Shah, V. P., J. P. Skelly, W. H. Barr, H. Malinowski, and G. L. Amidon, 1992, "Scale-up of Controlled Release Products - Preliminary Considerations," *Pharmaceutical Technology,* 16(5):35-40.

Shah, V. P., et al., 1995, "In Vivo Dissolution of Sparingly Water Soluble Drug Dosage Forms," *International Journal of Pharmaceutics,* 125:99-106.

Siewert, M., 1995, "FIP Guidelines for Dissolution Testing of Solid Oral Products," *Pharm. Ind.* 57:362-369.

Skelly, J. P., G. L. Amidon, W. H. Barr, L. Z. Benet, J. E. Carter, J. R. Robinson, V. P. Shah, and A. Yacobi, 1990, "In Vitro and In Vivo Testing and Correlation for Oral Controlled/Modified-Release Dosage Forms," *Pharmaceutical Research,* 7:975-982.

United States Pharmacopeia (USP), U.S. Pharmacopeial Convention, Inc. Rockville, MD.

EXHIBIT 7

EVONIK INDUSTRIES

D

Specification

Specifications and test methods for

EUDRAGIT® RL 30 D and EUDRAGIT® RS 30 D

"Ammonio Methacrylate Copolymer Type A" Ph. Eur.
"Ammonio Methacrylate Copolymer Type B" Ph. Eur.
"Ammonio Methacrylate Copolymer Dispersion, Type A and B" USP/NF
"Aminoalkylmethacrylate Copolymer RS" JPE

1 Commercial form

Aqueous dispersions of EUDRAGIT® RL 100 / EUDRAGIT® RS 100 with 30 % dry substance. The water is tested according to the specifications of "Purified Water in bulk" Ph. Eur. and according to the specifications for Conductivity of "Purified Water" USP. The dispersions contain 0.25 % sorbic acid Ph. Eur. / NF as a preservative as well as 0.1 % of sodium hydroxide Ph. Eur. / NF as an alkalizing agent.

EUDRAGIT® RL 30 D (Type A) and EUDRAGIT® RS 30 D (Type B) are described in the USP/NF monograph quoted above.

EUDRAGIT® RL 100 (Type A) and EUDRAGIT® RS 100 (Type B) are described in the Ph. Eur. and JPE monographs quoted above.

2 Chemical structure

EUDRAGIT® RL 100 and EUDRAGIT® RS 100 are copolymers of ethyl acrylate, methyl methacrylate and a low content of a methacrylic acid ester with quaternary ammonium groups (trimethylammonioethyl methacrylate chloride). The ammonium groups are present as salts and make the polymers permeable.

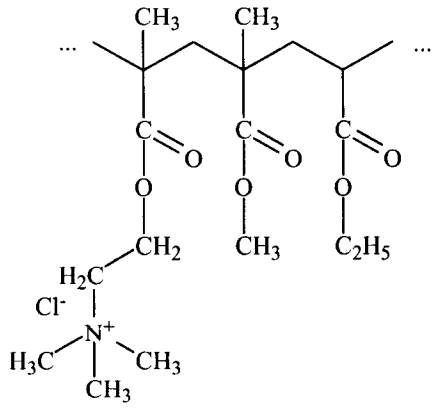

The average molecular weight is approx. 150,000.

3 Characters

Description

Milky-white liquids of low viscosity with a faint characteristic odour.

Solubility

The aqueous dispersions are miscible with water in any proportion, the milky-white appearance being retained. 1 part EUDRAGIT® RL 30 D / RS 30 D dissolves in 5 parts acetone, ethanol or isopropyl alcohol to give clear to slightly cloudy solutions.

When mixed with methanol in a ratio of 1:5, EUDRAGIT® RL 30 D dissolves completely, EUDRAGIT® RS 30 D only partially. When mixed with 1 N sodium hydroxide in a ratio of 1:2, none of the dispersions dissolve.

4 Tests

Film formation

10 g EUDRAGIT® RL 30 D / RS 30 D are mixed with 0.6 g triethyl citrate. When poured onto a glass plate, a transparent film forms upon evaporation of the water.

Dry substance / Residue on evaporation

28.5 - 31.5 %
The test is performed according to Ph. Eur. 2.2.32 method d.
1 g of the dispersions is dried in an oven for 3 hrs at 110 °C. After drying, the dispersion must form a transparent film.

Loss on drying

68.5 – 71.5 %
The test is performed according to "Dry substance / Residue on evaporation."

Assay

EUDRAGIT® RL 30 D: 10.18 - 13.73 % ammonio methacrylate units on dry substance (DS).
Alkali value: 27.5 - 37.1 mg KOH per g DS.
EUDRAGIT® RS 30 D: 6.11 - 8.26 % ammonio methacrylate units on DS.
Alkali value: 16.5 - 22.3 mg KOH per g DS.

The alkali value (AV) is defined similarly to the acid value. It states how many mg KOH are equivalent to the basic groups contained in 1 g dry substance (DS).

The assay is performed according to Ph. Eur. 2.2.20 "Potentiometric titration" or USP <541>.
2 g EUDRAGIT® RL 30 D or 4 g EUDRAGIT® RS 30 D are dried in vacuo in an oven for 30 minutes at 90 °C. Subsequently the sample is dissolved in 75 ml glacial acetic acid within about 30 minutes at approx. 50 °C. After the solution has cooled down, 25 ml copper (II) acetate solution (0.6 % solution in anhydrous acetic acid) are added and 0.1 N perchloric acid is used as the titrant.

$$\text{AV (mg KOH / g DS)} = \frac{\text{ml 0.1 N } HClO_4 \cdot 561}{\text{sample weight (g)} \cdot \text{DS (\%)}}$$

AV (mg KOH / g DS) = ammonio methacrylate units (%) · 2.701

Assay USP/NF: the test is performed according to the USP/NF monograph.
EUDRAGIT® RL 30 D: 10.18 - 13.73 % ammonio methacrylate units on DS
EUDRAGIT® RS 30 D: 6.11 – 8.26 % ammonio methacrylate units on DS

Viscosity / Apparent viscosity

Max. 100 mPa · s
The viscosity of the dispersions is determined by means of a Brookfield viscometer (spindle 1 / 30 rpm / 20 °C).

pH

4.0 – 6.0
The pH is determined according to Ph. Eur. 2.25.

Relative density

d_{20}^{20}: 1.047 - 1.057
The relative density of the dispersions is determined according to Ph. Eur. 2.2.5.

Coagulum content

Max. 1,000 mg / 100 g
A stainless steel wire cloth with a mesh size of 0.125 mm (mesh number 125, ISO) is accurately weighed. 100 g of the dispersions are filtered through this cloth, which is then washed with water until a clear filtrate is obtained, dried to constant weight at 105 °C and weighed to determine the filtration residue.

5 Purity

Sulphated ash / Residue on ignition

Max. 0.5 %
The test is performed according to Ph. Eur. 2.4.14 or USP <281>.
1 g of the dispersions is used for the test.

Heavy metals

Max. 20 ppm
The test is performed according to Ph. Eur. 2.4.8 method C or USP <231> method II.
1 g of the dispersions is used for the test.

Methanol

Max. 1.0 %
The test is performed on according to Ph. Eur. 2.4.24, sample preparation 2.
0.200 g is used for the test.

Monomers

Ethyl acrylate: max. 30 ppm
Methyl methacrylate: max. 20 ppm
The test is performed according to the Ph. Eur. or USP/NF Monograph.

Microbial count

Total aerobic microbial count (TAMC): max. 1,000 CFU / g
Total combined yeasts and moulds count (TYMC): max. 100 CFU / g
(Acceptance criteria according to Ph. Eur. 5.1.4 / USP 1111)
The test is performed according to Ph. Eur. 2.6.12 or USP <61>.

6 Identity testing

First identification

The material must comply with the tests for "Assay" and "Viscosity / Apparent viscosity."

Second identification

IR spectroscopy on a dry film approx. 15 µm thick. The film is obtained by applying one drop of EUDRAGIT® RL 30 D / RS 30 D to a glass plate and covering with a water-resistant crystal disc (AgCl, KRS 5). By lightly pressing on and then removing the crystal disc, a clear film is obtained after a drying period of about 15 minutes at 60 °C.

The figures on page 4 show the characteristic bands of the ester groups at 1,150 - 1,190 and 1,240 and 1,270 cm^{-1}, as well as the C = O ester vibration at 1,730 cm^{-1}. In addition, CH_X vibrations can be discerned at 1,385, 1,450, 1,475 and 2,950 - 3,000 cm^{-1}.

A small absorption at 1,570 cm^{-1} is caused by the sorbic acid.

EVONIK INDUSTRIES

EUDRAGIT® RL 30 D

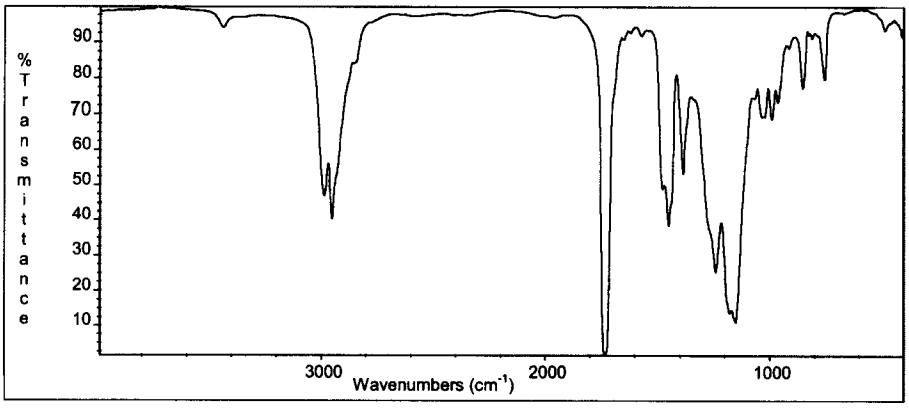

EUDRAGIT® RS 30 D

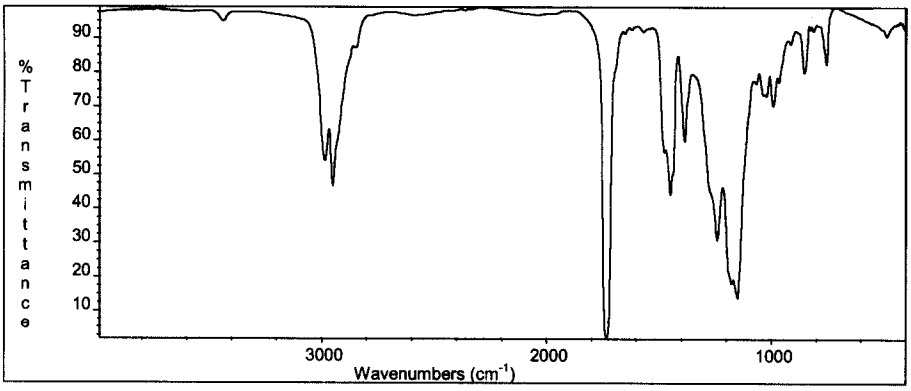

7 Detection in dosage forms

The dosage forms are extracted using the solvents listed under "Solubility" if necessary after crushing. Insoluble substances are isolated by filtration or centrifugation. The clear filtrate is boiled down and the residue identified by IR spectroscopy.

8 Storage

EUDRAGIT® RL 30 D: Store at temperatures up to 25 °C. Protect from freezing. Any storage between 8°C and 25°C fulfils this requirement.

EUDRAGIT® RS 30 D: Store at controlled room temperatures (USP, General Notices). Protect from freezing. Any storage between 8°C and 25°C fulfils this requirement.

Avoid contamination during sampling. Containers that have been opened for use should be closed again immediately and the content used up within the next few weeks.

9 Stability

Minimum stability dates are given on the product labels and batch-related Certificates of Analysis. Storage Stability data are available upon request.

EVONIK Röhm GmbH
Pharma Polymers
Kirschenallee
64293 Darmstadt
Phone: +49 (0) 6151/18-4019
Fax: +49 (0) 6151/18-3520
e-mail: pharma.polymers@evonik.com
Internet: www.pharma-polymers.com